technique as having lung cancer are often at advanced clinical stages already.

In contrast, *EML4–ALK*-positive cells may be detected in a very sensitive way. As *EML4* and *ALK* are mapped to chromosome 2p in opposite directions in normal cells, a set of PCR primers (one at exon 13 of *EML4* and the other at exon 20 of *ALK*; Fig. 3a) will not generate any specific PCR products from cDNA of normal cells or of cancer without inv(2)(p21p23). Therefore, RT-PCR of the cDNA (or PCR of the genome fusion points) should become a highly sensitive yet reliable detection method for EML4–ALK-positive tumors. Given the high sensitivity of PCR, it is even expected that one cancer cell out of 10^5–10^6 normal cells in sputa may be detected, which would significantly help to identify individuals with lung cancer at early resectable stages. Soda *et al.* indeed succeeded in capturing 10 cells/mL of EML4–ALK-positive cells in sputum by RT-PCR.[13] It would therefore be of great importance to test the idea that such RT-PCR-based detection with sputa may be useful as a general screening method for early stages of NSCLC (among individuals with chronic cough or sputa, for instance).

Once detected with such screening systems, individuals positive for *EML4–ALK* may undergo surgical resection of tumors or receive chemotherapies with compounds that specifically suppress ALK activity. Just like the case of *BCR–ABL1* in CML, *EML4–ALK* detection will likely play a pivotal role in the diagnosis of NSCLC positive for the fusion gene. In this regard, it is mandatory that every *EML4–ALK*-positive tumor be identified accurately by the diagnostic PCR system. There is a caveat, however, that the break and fusion points within the *EML4* and *ALK* loci may be more divergent than previously appreciated.

Soda *et al.* first discovered two variants of *EML4–ALK*: exon 13 of *EML4* fused to exon 20 of *ALK* in variant 1, and exon 20 of *ELM4* fused to exon 20 of *ALK* in variant 2.[13] In addition, we and Pasi A. Jänne and colleagues (Dana-Farber Cancer Institute) have recently identified two more variants (variants 3a and 3b, which connect exons 6a and 6b, respectively, of *EML4* to exon 20 of *ALK*) (Fig. 3b).[14,45] Further variants that connect various exons of *EML4* to *ALK* are being identified by a number of groups worldwide.[44–46]

In addition to exons 6 (variant 3), 13 (variant 1), and 20 (variant 2) of *EML4*, an in-frame fusion to exon 20 of *ALK* can occur with exon 2, 18, or 21 of *EML4* (Fig. 3b). Given that the amino-terminal coiled coil domain of EML4 is responsible for the oligomerization of EML4–ALK (see below) and that exon 2 of *EML4* encodes the entire coiled coil domain, all of these possible fusion genes would encode EML4–ALK proteins containing the coiled coil domain and therefore likely produce oncogenic EML4–ALK kinases. To screen for all variants (both known and unknown) of *EML4–ALK* and to estimate the frequency of such oncogenes in human cancers, Takeuchi *et al.* have developed a single-tube multiplex RT-PCR system that captures all possible in-frame fusions between *EML4* and *ALK*.[46] From screening of lung adenocarcinoma specimens ($n = 253$), they have identified a total of 11 samples (4.35%) carrying variants 1, 2, 3, or unknown isoforms (referred to as variants 4 and 5) of *EML4–ALK*.

Unexpectedly, in one of the new isoforms (variant 4), exon 14 of *EML4* is connected to an unknown sequence of 11 bp, and further fused to a nucleotide at position 50 of exon 20 of *ALK*. Although exon 14 of *EML4* is not expected to produce an in-frame fusion to exon 20 of *ALK*, insertion of the unknown 11-bp sequence and its ligation to a position within the *ALK* exon allows an in-frame connection between the two genes.

Additionally, exon 2 of *EML4* is fused to exon 20 of *ALK* or to a nucleotide 117 bp upstream of exon 20 of *ALK*, giving rise to variants 5a and 5b of *EML4–ALK*, respectively. Takeuchi *et al.* further successfully isolated full-length cDNA for variants 4, 5a, and 5b of EML4–ALK, and confirmed the transforming potential of all isoforms.[46] Takeuchi *et al.* have also screened for *EML4–ALK* cDNA, with the same multiplex RT-PCR technique, among other solid tumors ($n = 403$) including squamous cell carcinoma ($n = 71$) and small cell carcinoma ($n = 21$) of the lung. Interestingly, none of these tumors were positive for the fusion cDNA, indicating specificity of the *EML4–ALK* oncogene to lung cancer (especially adenocarcinoma).

Similarly, Wong *et al.* have tried to identify all possible in-frame fusions between *EML4* and *ALK* among a panel of NSCLC specimens ($n = 240$), discovering 13 cases (5.42%) positive for variants 1, 2, 3, and an unknown isoform of *EML4–ALK*.[44] Notably, variant 3 was the most frequent isoform ($n = 8$) in their Chinese cohort. Based on these data, the proportion of EML4–ALK-positive tumors in NSCLC seems to be ~5% in the Asian ethnic group, and may be lower in the others.[44,46,47]

It should be noted that all subtypes of EML4–ALK have not always been assayed in the published screenings and, further, that there may still be other variants not yet discovered. Therefore, to estimate the true prevalence of EML4–ALK-positive tumors within a given ethnic group, it is necessary to examine, in large cohorts, all possible in-frame fusions between *EML4* and *ALK* among the subjects. Additionally, given the increasing number of *EML4–ALK* variants, I personally hope that researchers may, in the near future, develop a more reasonable and uniform nomenclature system for such variants (E13; A20 for variant 1, and E6a; A20 for variant 3a, for instance) than the current one (variants 1, 2, 3, etc).

With regard to other diagnostic tools for EML4–ALK-positive tumors, immunohistochemical detection of EML4–ALK proteins in specimens obtained by biopsy or surgical resection would be a convenient screening system in clinics. In anaplastic large cell lymphoma, such screening with antibodies to the intracellular region of ALK has been used routinely to detect lymphoma positive for NPM–ALK.[48] Unfortunately, however, it is often difficult to stain EML4–ALK with such antibodies in NSCLC that are positive for *EML4–ALK* mRNA (K. Takeuchi and K. Inamura, personal communication). This discrepancy may be due to: (i) the weaker promoter activity of the *EML4* gene (which drives the expression of *EML4–ALK*) compared to that of *NPM* (which drives the expression of *NPM–ALK*), or (ii) a lower stability of the EML4–ALK protein than that of NPM–ALK. Further improvements in the sensitivity of immunohistochemical detection of EML4–ALK would be desirable to apply such systems to routine pathological screenings.

Transforming activity of EML4–ALK

How does fusion to EML4 induce a marked transforming potential in ALK? A number of fusion-type PTK carry an oligomerization motif within the fusion partner regions, which thereby leads to dimerization and autophosphorylation of the corresponding kinase domain.[49,50] Consistent with this notion, the NPM region in the NPM–ALK protein was shown to be essential in the oligomerization and transforming potential of this fusion kinase (Fig. 2).[51] Similarly, TPM3–ALK and TPM4–ALK found in IMT and EML4–ALK in NSCLC all carry a coiled coil domain within the fusion partners, which may act as an oligomerization motif. Indeed, EML4–ALK homodimerizes in cells, but internal deletion of the basic domain of EML4 (which contains the coiled coil domain) severely hampers such physical association. Accordingly, this mutant form of EML4–ALK loses its marked tumor-formation activity *in vivo*, and has decreased tyrosine kinase activity *in vitro*.[13] It should be noted, however, that truncation of subdomains other than the coiled coil domain of EML4–ALK also affects its transforming potential, suggesting that self-oligomerization is not the only mechanism to induce oncogenic potential in EML4–ALK.[13]

As wild-type ALK is a PTK with a single transmembrane region, it is presumed that the *in vivo* function of ALK is that of

doi: 10.1111/j.1349-7006.2008.00972.x

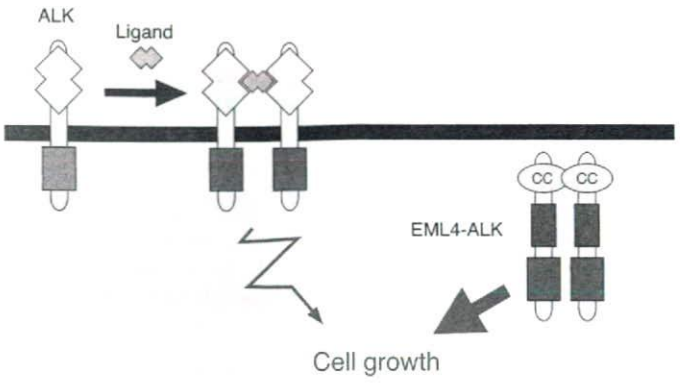

Fig. 4. Activation mechanisms for anaplastic lymphoma kinase (ALK) and echinoderm microtubule-associated protein like-4 (EML4)–ALK. Wild-type ALK is thought to undergo transient homodimerization in response to binding of a specific ligand, resulting in its activation and mitogenic signal transduction. In contrast, EML4–ALK is constitutively oligomerized via the coiled coil domain (CC) of EML4, resulting in persistent mitogenic signaling that eventually leads to malignant transformation.

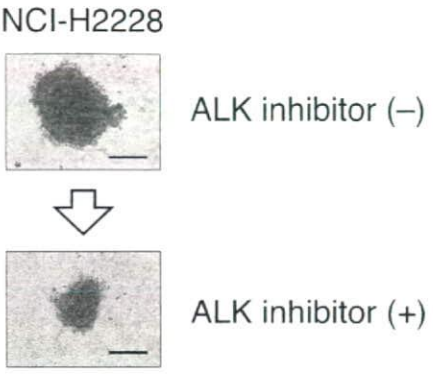

Fig. 5. Suppression of the growth of an echinoderm microtubule-associated protein like-4 (EML4)–anaplastic lymphoma kinase (ALK)-positive cell line with an ALK inhibitor. The non-small cell lung cancer cell line NCI-H2228, which is positive for *EML4–ALK* (variant 3), was maintained in spheroid culture for 2 days and was photographed after an additional 5 days of incubation in the absence (upper panel) or presence (lower panel) of 5 nmol/L 2,4-pyrimidinediamine.[14] Scale bars = 4 mm.

a cell surface receptor for specific ligands (probably growth factors). Unfortunately, however, such ligands have not been isolated in mammals. In *Drosophila melanogaster*, a protein homologous to human and mouse ALK is expressed in visceral mesoderm in the embryo, and malfunctions in Alk lead to visceral mesoderm defects in early embryogenesis, which resembles the phenotype of dysfunction in a secreted protein, jelly belly (Jeb). Upon binding to Jeb, Alk becomes activated to trigger the Ras–mitogen-activated protein kinase cascade and transcriptional activation of a subset of genes,[52] suggesting that Jeb is the ligand of Alk in fly.

In mammals, however, pleiotrophin[53] and midkine[54] are proposed ligands of ALK and are expressed specifically in brain and spinal cord.[55,56] Pleiotrophin may bind ALK at a low dissociation constant and induce tyrosine phosphorylation on ALK as well as putative downstream effector molecules.[53] However, other cellular receptors for pleiotrophin have also been identified and, hence, it is not yet clear if the observed effects of pleiotrophin are mediated mainly through ALK.[57,58]

Although it is theoretically possible that the extracellular region of ALK may act as its own ligand, the Jeb–Alk interaction in fly suggests that ALK likely functions as a cellular receptor for specific ligands in mammalian cells as well. Presumably, upon ligand binding (and only upon such binding), ALK becomes oligomerized and activated to trigger a transient growth signal in cells (Fig. 4). However, EML4–ALK and other ALK fusion proteins are constitutively oligomerized through the binding motif within the corresponding fusion partners, and activated to maintain a persistent mitogenic signal that finally leads to tumor formation.

A pivotal role of ALK fusion proteins in malignant transformation has been demonstrated clearly in the case of NPM–ALK. Retroviral transduction of NPM–ALK mRNA in bone marrow cells induces lymphoma-like disorders in mice,[59,60] and transgenic mice with *Vav* promoter-driven expression of *NPM–ALK* results in the generation of lymphoma.[61] Furthermore, injected lymphoma cells positive for *NPM–ALK* were effectively eradicated from mice by treatment with a specific inhibitor against ALK,[40] suggesting that the activated kinase potential of NPM–ALK is central to the lymphomagenesis.

A few experiments also support such a pivotal role for EML4–ALK in lung cancer. Koivunen *et al.* have found that treatment with a specific inhibitor for ALK (TAE684) induces rapid cell death of one NSCLC cell line (NCI-H3122) in culture, which harbors variant 1 of *EML4–ALK*.[45] Another NSCLC cell line, NCI-H2228, was shown to be positive for variant 3 of *EML4–ALK*, but TAE684 treatment failed to induce drastic effects in this these cells. However, McDermott *et al.* did find partial inhibition of cell viability (66% reduction compared to the control experiments) in NCI-H2228 after treatment with TAE684, as well as in NCI-H3122 (75% reduction).[62] Similarly, we found marked growth suppression of NCI-H2228 with an ALK inhibitor only in a spheroid culture system (Fig. 5),[14] not in a regular *in vitro* culture. These data thus indicate that EML4–ALK may be the principle transforming protein in some NSCLC cells (such as NCI-H3122) that are therefore fully sensitive to ALK inhibitors. However, it is likely that at least one other potential transforming protein is present with EML4–ALK in other NSCLC (e.g. NCI-H2228), and thus inhibition of ALK enzymatic activity provides significant but incomplete growth suppression.

With regard to the *in vivo* role of EML4–ALK, it is important to test if EML4–ALK activity can induce lung cancer *in vivo*. To address this issue, Soda *et al.* have recently generated transgenic mice in which EML4–ALK mRNA is transcribed specifically in lung epithelial cells by the use of a promoter fragment of the surfactant protein C gene.[63] Surprisingly, all independent lines of such mice develop hundreds of adenocarcinoma nodules in both lungs at only a few weeks after birth, proving for the first time the marked transforming activity of EML4–ALK *in vivo* (Soda *et al.*, unpublished data). More importantly, treatment of such mice with a chemical compound that suppresses ALK activity rapidly cleared those nodules from the lungs. Therefore, it is likely that EML4–ALK-positive lung cancer cells are at least partially dependent on their PTK activity for growth, and any means to suppress this activity would be a promising strategy for treating this intractable disorder.

Concluding remarks

The data from *EML4–ALK* transgenic mice clearly show the central role of this fusion kinase in lung cancer, and such mice also provide an efficient *in vivo* screening system for ALK inhibitors. Recently, treatment with an ALK inhibitor was shown to suppress or inhibit the growth of some neuroblastoma cell lines, in addition to NSCLC and anaplastic large cell lymphoma.[62,64] Because the *EML4–ALK* and *NPM–ALK* fusion genes are present in the latter two, such inhibitor-sensitive neuroblastoma cell lines may also possess other *ALK* mutants. These data suggest that tumors of any tissue origin may be treated with the same ALK inhibitors provided that they carry any one of the

oncogenic ALK mutants. Therefore, 'ALKoma'[65,66] may form a novel clinical entity as is the case for v-kit Hardy-Zuckerman 4 feline sarcoma viral oncogene homolog (KIT) mutant-positive tumors in acute myeloid leukemia, mastocytosis,[67,68] and gastrointestinal stromal tumor.[69]

However, given the marked diversity in the sensitivity of EML4–ALK-positive cell lines to ALK inhibitors,[45,62] identification of coexisting oncogenes in ALK mutant-positive tumors would be valuable to increase the efficacy of treatments with ALK inhibitors.

Furthermore, as various ALK fusion proteins have divergent subcellular localizations (probably dependent on the nature of fusion partner proteins),[46,70] downstream signaling pathways may vary among them. Indeed, although signal transducer and activator of transcription (STAT) proteins likely play a key role in the mitogenic signaling of NPM–ALK, such a role is unlikely for EML4–ALK[46,71] and some other ALK fusions.[70] It is therefore of great clinical relevance to decipher the profiles of oncogenes or tumor-suppressor genes and downstream proteins for each ALK fusion in each cancer subtype.

Acknowledgments

I apologize to all of the authors whose work could not be included in this manuscript owing to space constraints. I thank the members of our laboratory for their support and excellent work, and Yuichi Ishikawa and Kengo Takeuchi for helpful suggestions and discussion. This work was supported in part by a grant for Research on Human Genome Tailor-made from the Ministry of Health, Labor, and Welfare of Japan, and by a Grant-in-Aid for Scientific Research on Priority Areas from the Ministry of Education, Culture, Sports, Science, and Technology of Japan.

References

1 Futreal PA, Coin L, Marshall M *et al.* A census of human cancer genes. *Nat Rev Cancer* 2004; **4**: 177–83.
2 Ren R. Mechanisms of BCR-ABL in the pathogenesis of chronic myelogenous leukaemia. *Nat Rev Cancer* 2005; **5**: 172–83.
3 Li S, Ilaria RL Jr, Million RP, Daley GQ, Van Etten RA. The P190, P210, and P230 forms of the BCR/ABL oncogene induce a similar chronic myeloid leukemia-like syndrome in mice but have different lymphoid leukemogenic activity. *J Exp Med* 1999; **189**: 1399–412.
4 Pear WS, Miller JP, Xu L *et al.* Efficient and rapid induction of a chronic myelogenous leukemia-like myeloproliferative disease in mice receiving P210 bcr/abl-transduced bone marrow. *Blood* 1998; **92**: 3780–92.
5 Oehler VG, Radich JP. Monitoring bcr-abl by polymerase chain reaction in the treatment of chronic myeloid leukemia. *Curr Oncol Rep* 2003; **5**: 426–35.
6 Druker BJ, Talpaz M, Resta DJ *et al.* Efficacy and safety of a specific inhibitor of the BCR-ABL tyrosine kinase in chronic myeloid leukemia. *N Engl J Med* 2001; **344**: 1031–7.
7 Druker BJ, Guilhot F, O'Brien SG *et al.* Five-year follow-up of patients receiving imatinib for chronic myeloid leukemia. *N Engl J Med* 2006; **355**: 2408–17.
8 Mitelman F. Recurrent chromosome aberrations in cancer. *Mutat Res* 2000; **462**: 247–53.
9 Jemal A, Siegel R, Ward E, Murray T, Xu J, Thun MJ. Cancer statistics, 2007. *CA Cancer J Clin* 2007; **57**: 43–66.
10 Mitelman F, Mertens F, Johansson B. Prevalence estimates of recurrent balanced cytogenetic aberrations and gene fusions in unselected patients with neoplastic disorders. *Genes Chromosomes Cancer* 2005; **43**: 350–66.
11 Mitelman F, Johansson B, Mertens F. Fusion genes and rearranged genes as a linear function of chromosome aberrations in cancer. *Nat Genet* 2004; **36**: 331–4.
12 Mitelman F, Johansson B, Mertens F. The impact of translocations and gene fusions on cancer causation. *Nat Rev Cancer* 2007; **7**: 233–45.
13 Soda M, Choi YL, Enomoto M *et al.* Identification of the transforming *EML4–ALK* fusion gene in non-small-cell lung cancer. *Nature* 2007; **448**: 561–6.
14 Choi YL, Takeuchi K, Soda M *et al.* Identification of novel isoforms of the *EML4–ALK* transforming gene in non-small cell lung cancer. *Cancer Res* 2008; **68**: 4971–6.
15 Inamura K, Takeuchi K, Togashi Y *et al. EML4–ALK* fusion is linked to histological characteristics in a subset of lung cancers. *J Thorac Oncol* 2008; **3**: 13–17.
16 Tomlins SA, Rhodes DR, Perner S *et al.* Recurrent fusion of TMPRSS2 and ETS transcription factor genes in prostate cancer. *Science* 2005; **310**: 644–8.
17 Tomlins SA, Laxman B, Dhanasekaran SM *et al.* Distinct classes of chromosomal rearrangements create oncogenic ETS gene fusions in prostate cancer. *Nature* 2007; **448**: 595–9.
18 Kumar-Sinha C, Tomlins SA, Chinnaiyan AM. Recurrent gene fusions in prostate cancer. *Nat Rev Cancer* 2008; **8**: 497–511.
19 Lynch TJ, Bell DW, Sordella R *et al.* Activating mutations in the epidermal growth factor receptor underlying responsiveness of non-small-cell lung cancer to gefitinib. *N Engl J Med* 2004; **350**: 2129–39.
20 Menard S, Pupa SM, Campiglio M, Tagliabue E. Biologic and therapeutic role of HER2 in cancer. *Oncogene* 2003; **22**: 6570–8.
21 Sharma SV, Settleman J. Oncogene addiction: setting the stage for molecularly targeted cancer therapy. *Genes Dev* 2007; **21**: 3214–31.
22 Goldfarb M, Shimizu K, Perucho M, Wigler M. Isolation and preliminary characterization of a human transforming gene from T24 bladder carcinoma cells. *Nature* 1982; **296**: 404–9.
23 Aaronson SA. Growth factors and cancer. *Science* 1991; **254**: 1146–53.
24 Choi YL, Moriuchi R, Osawa M *et al.* Retroviral expression screening of oncogenes in natural killer cell leukemia. *Leuk Res* 2005; **29**: 943–9.
25 Fujiwara S, Yamashita Y, Choi YL *et al.* Transforming activity of the lymphotoxin-β receptor revealed by expression screening. *Biochem Biophys Res Commun* 2005; **338**: 1256–62.
26 Kisanuki H, Choi YL, Wada T *et al.* Retroviral expression screening of oncogenes in pancreatic ductal carcinoma. *Eur J Cancer* 2005; **41**: 2170–5.
27 Choi YL, Kaneda R, Wada T *et al.* Identification of a constitutively active mutant of JAK3 by retroviral expression screening. *Leuk Res* 2007; **31**: 203–9.
28 Fujiwara S, Yamashita Y, Choi YL *et al.* Transforming activity of purinergic receptor P2Y, G protein coupled, 8 revealed by retroviral expression screening. *Leuk Lymphoma* 2007; **48**: 978–86.
29 Hatanaka H, Takada S, Choi YL *et al.* Transforming activity of purinergic receptor P2Y, G-protein coupled, 2 revealed by retroviral expression screening. *Biochem Biophys Res Commun* 2007; **356**: 723–6.
30 Kitamura T, Onishi M, Kinoshita S, Shibuya A, Miyajima A, Nolan GP. Efficient screening of retroviral cDNA expression libraries. *Proc Natl Acad Sci USA* 1995; **92**: 9146–50.
31 Yoshizuka N, Moriuchi R, Mori T *et al.* An alternative transcript derived from the trio locus encodes a guanosine nucleotide exchange factor with mouse cell-transforming potential. *J Biol Chem* 2004; **279**: 43 998–4004.
32 American Cancer Society. Global Cancer Facts and Figures 2007. [Cited 18 October, 2008.] Available from URL: http://www.cancer.org/downloads/STT/Global_Facts_and_Figures_2007_rev2.pdf.
33 Shigematsu H, Lin L, Takahashi T *et al.* Clinical and biological features associated with epidermal growth factor receptor gene mutations in lung cancers. *J Natl Cancer Inst* 2005; **97**: 339–46.
34 Schiller JH, Harrington D, Belani CP *et al.* Comparison of four chemotherapy regimens for advanced non-small-cell lung cancer. *N Engl J Med* 2002; **346**: 92–8.
35 Pollmann M, Parwaresch R, Adam-Klages S, Kruse ML, Buck F, Heidebrecht HJ. Human EML4, a novel member of the EMAP family, is essential for microtubule formation. *Exp Cell Res* 2006; **312**: 3241–51.
36 Morris SW, Naeve C, Mathew P *et al.* ALK, the chromosome 2 gene locus altered by the t(2;5) in non-Hodgkin's lymphoma, encodes a novel neural receptor tyrosine kinase that is highly related to leukocyte tyrosine kinase (LTK). *Oncogene* 1997; **14**: 2175–88.
37 Morris SW, Kirstein MN, Valentine MB *et al.* Fusion of a kinase gene, ALK, to a nucleolar protein gene, NPM, in non-Hodgkin's lymphoma. *Science* 1994; **263**: 1281–4.
38 Shiota M, Fujimoto J, Semba T, Satoh H, Yamamoto T, Mori S. Hyperphosphorylation of a novel 80 kDa protein-tyrosine kinase similar to Ltk in a human Ki-1 lymphoma cell line, AMS3. *Oncogene* 1994; **9**: 1567–74.
39 Wan W, Albom MS, Lu L *et al.* Anaplastic lymphoma kinase activity is essential for the proliferation and survival of anaplastic large-cell lymphoma cells. *Blood* 2006; **107**: 1617–23.
40 Galkin AV, Melnick JS, Kim S *et al.* Identification of NVP-TAE684, a potent, selective, and efficacious inhibitor of NPM-ALK. *Proc Natl Acad Sci USA* 2007; **104**: 270–5.
41 Pulford K, Morris SW, Turturro F. Anaplastic lymphoma kinase proteins in growth control and cancer. *J Cell Physiol* 2004; **199**: 330–58.
42 Lacronique V, Boureux A, Valle VD *et al.* A TEL-JAK2 fusion protein with constitutive kinase activity in human leukemia. *Science* 1997; **278**: 1309–12.
43 Shinmura K, Kageyama S, Tao H *et al.* EML4–ALK fusion transcripts, but no NPM–, TPM3–, CLTC–, ATIC–, or TFG–ALK fusion transcripts, in non-small cell lung carcinomas. *Lung Cancer* 2008; **61**: 163–9.
44 Wong DD-S, So KK-T, Leung EL-H *et al.* EML4–ALK is a new oncogene in non-small cell lung carcinoma showing wild-type EGFR and K-RAS from

doi: 10.1111/j.1349-7006.2008.00972.x

non-smokers. *American Association of Cancer Research Annual Meeting* 12–16 April, 2008, San Diego, AACR (Philadelphia): (poster #LB-62).
45 Koivunen JP, Mermel C, Zejnullahu K *et al.* EML4–ALK fusion gene and efficacy of an ALK kinase inhibitor in lung cancer. *Clin Cancer Res* 2008; **14**: 4275–83.
46 Takeuchi K, Choi YL, Soda M *et al.* Multiplex RT-PCR screening for EML4-ALK fusion transcripts. *Clin Cancer Res* 2008; **14**: 6618–24.
47 Perner S, Wagner PL, Demichelis F *et al.* EML4–ALK fusion lung cancer: a rare acquired event. *Neoplasia* 2008; **10**: 298–302.
48 Cataldo KA, Jalal SM, Law ME *et al.* Detection of t(2;5) in anaplastic large cell lymphoma: comparison of immunohistochemical studies, FISH, and RT-PCR in paraffin-embedded tissue. *Am J Surg Pathol* 1999; **23**: 1386–92.
49 Turner SD, Alexander DR. Fusion tyrosine kinase mediated signalling pathways in the transformation of haematopoietic cells. *Leukemia* 2006; **20**: 572–82.
50 Matsumura I, Mizuki M, Kanakura Y. Roles for deregulated receptor tyrosine kinases and their downstream signaling molecules in hematologic malignancies. *Cancer Sci* 2008; **99**: 479–85.
51 Bischof D, Pulford K, Mason DY, Morris SW. Role of the nucleophosmin (NPM) portion of the non-Hodgkin's lymphoma-associated NPM–anaplastic lymphoma kinase fusion protein in oncogenesis. *Mol Cell Biol* 1997; **17**: 2312–25.
52 Lee HH, Norris A, Weiss JB, Frasch M. Jelly belly protein activates the receptor tyrosine kinase Alk to specify visceral muscle pioneers. *Nature* 2003; **425**: 507–12.
53 Stoica GE, Kuo A, Aigner A *et al.* Identification of anaplastic lymphoma kinase as a receptor for the growth factor pleiotrophin. *J Biol Chem* 2001; **276**: 16 772–9.
54 Stoica GE, Kuo A, Powers C *et al.* Midkine binds to anaplastic lymphoma kinase (ALK) and acts as a growth factor for different cell types. *J Biol Chem* 2002; **277**: 35 990–8.
55 Pulford K, Lamant L, Morris SW *et al.* Detection of anaplastic lymphoma kinase (ALK) and nucleolar protein nucleophosmin (NPM)–ALK proteins in normal and neoplastic cells with the monoclonal antibody ALK1. *Blood* 1997; **89**: 1394–404.
56 Iwahara T, Fujimoto J, Wen D *et al.* Molecular characterization of ALK, a receptor tyrosine kinase expressed specifically in the nervous system. *Oncogene* 1997; **14**: 439–49.
57 Maeda N, Nishiwaki T, Shintani T, Hamanaka H, Noda M. 6B4 proteoglycan/phosphacan, an extracellular variant of receptor-like protein-tyrosine phosphatase zeta/RPTPbeta, binds pleiotrophin/heparin-binding growth-associated molecule (HB-GAM). *J Biol Chem* 1996; **271**: 21 446–52.
58 Raulo E, Chernousov MA, Carey DJ, Nolo R, Rauvala H. Isolation of a neuronal cell surface receptor of heparin binding growth-associated molecule (HB-GAM). Identification as N-syndecan (syndecan-3). *J Biol Chem* 1994; **269**: 12 999–3004.
59 Kuefer MU, Look AT, Pulford K *et al.* Retrovirus-mediated gene transfer of NPM–ALK causes lymphoid malignancy in mice. *Blood* 1997; **90**: 2901–10.
60 Miething C, Grundler R, Fend F *et al.* The oncogenic fusion protein nucleophosmin–anaplastic lymphoma kinase (NPM–ALK) induces two distinct malignant phenotypes in a murine retroviral transplantation model. *Oncogene* 2003; **22**: 4642–7.
61 Turner SD, Tooze R, Maclennan K, Alexander DR. Vav-promoter regulated oncogenic fusion protein NPM–ALK in transgenic mice causes B-cell lymphomas with hyperactive Jun kinase. *Oncogene* 2003; **22**: 7750–61.
62 McDermott U, Iafrate AJ, Gray NS *et al.* Genomic alterations of anaplastic lymphoma kinase may sensitize tumors to anaplastic lymphoma kinase inhibitors. *Cancer Res* 2008; **68**: 3389–95.
63 Zhao B, Magdaleno S, Chua S *et al.* Transgenic mouse models for lung cancer. *Exp Lung Res* 2000; **26**: 567–79.
64 McDermott U, Sharma SV, Dowell L *et al.* Identification of genotype-correlated sensitivity to selective kinase inhibitors by using high-throughput tumor cell line profiling. *Proc Natl Acad Sci USA* 2007; **104**: 19 936–41.
65 Ponzoni M, Terreni MR, Ciceri F *et al.* Primary brain CD30$^+$ ALK1$^+$ anaplastic large cell lymphoma ('ALKoma'): the first case with a combination of 'not common' variants. *Ann Oncol* 2002; **13**: 1827–32.
66 Chiarle R, Voena C, Ambrogio C, Piva R, Inghirami G. The anaplastic lymphoma kinase in the pathogenesis of cancer. *Nat Rev Cancer* 2008; **8**: 11–23.
67 Longley J, Duffy TP, Kohn S. The mast cell and mast cell disease. *J Am Acad Dermatol* 1995; **32**: 545–61.
68 Furitsu T, Tsujimura T, Tono T *et al.* Identification of mutations in the coding sequence of the proto-oncogene c-kit in a human mast cell leukemia cell line causing ligand-independent activation of c-kit product. *J Clin Invest* 1993; **92**: 1736–44.
69 Siehl J, Thiel E. C-kit, GIST, and imatinib. *Recent Results Cancer Res* 2007; **176**: 145–51.
70 Armstrong F, Duplantier MM, Trempat P *et al.* Differential effects of X-ALK fusion proteins on proliferation, transformation, and invasion properties of NIH3T3 cells. *Oncogene* 2004; **23**: 6071–82.
71 Rikova K, Guo A, Zeng Q *et al.* Global survey of phosphotyrosine signaling identifies oncogenic kinases in lung cancer. *Cell* 2007; **131**: 1190–203.

Genome-wide histone methylation profile for heart failure

Ruri Kaneda[1,2], Shuji Takada[1], Yoshihiro Yamashita[1], Young Lim Choi[1], Mutsuko Nonaka-Sarukawa[2], Manabu Soda[1], Yoshio Misawa[3], Tadashi Isomura[4], Kazuyuki Shimada[2] and Hiroyuki Mano[1,5,*]

Divisions of [1]Functional Genomics, Jichi Medical University, Tochigi 329-0498, Japan
[2]Cardiovascular Medicine, Jichi Medical University, Tochigi 329-0498, Japan
[3]Cardiovascular Surgery, Jichi Medical University, Tochigi 329-0498, Japan
[4]Hayama Heart Center, Kanagawa 240-0116, Japan
[5]CREST, Japan Science and Technology Agency, Saitama 332-0012, Japan

Epigenetic alterations are implicated in the development of cardiac hypertrophy and heart failure, but little is known of which epigenetic changes in which regions of the genome play such a role. We now show that trimethylation of histone H3 on lysine-4 (K4TM) or lysine-9 (K9TM) is markedly affected in cardiomyocytes in association with the development of heart failure in a rat disease model. High-throughput pyrosequencing performed with ChIP products for K4TM or K9TM prepared from human left ventricular tissue with retained or damaged function also revealed that protein-coding genes located in the vicinity of K4TM marks differ between functional and disabled myocytes, yet both sets of genes encode proteins that function in the same signal transduction pathways for cardiac function, indicative of differential K4TM marking during the development of heart failure. However, K9TM mark-profile was less dependent on the disease status compared to that of K4TM. Our data collectively reveal global epigenetic changes in cardiac myocytes associated with heart failure.

Introduction

A variety of conditions, including pressure or volume overload in the cardiovascular system and remodeling of the left ventricle of the heart after ischemic damage, result in heart failure, which is characterized by a reduction in contractile ability and a decrease in the number of viable myocytes in the heart (James *et al.* 2000). Treatment of heart failure remains problematic, and this condition is thus still one of the leading causes of human death (Braunwald 1997).

Epigenetic status has been linked to cardiac hypertrophy and heart failure. The histone acetyltransferase activity of CREB-binding protein (CBP) and p300 is thus required for the induction of hypertrophic changes in cardiac muscle cells by phenylephrine (Gusterson *et al.* 2003). Consistent with this observation, inhibition of histone deacetylase (HDAC) activity results in an increase in the size of cardiac muscle cells (Iezzi *et al.* 2004). Furthermore, HDACs of class II (HDAC4, -5, -7, and -9) suppress cardiac hypertrophy in part by binding to and inhibiting the activity of myocyte enhancer factor 2 (Zhang *et al.* 2002). Induction of the atrial natriuretic peptide gene is associated with acetylation of histones (H3 and H4) located in the 3′ untranslated region of the gene (Kuwahara *et al.* 2001). Histones bound to the β-myosin heavy chain gene have also been shown to be targeted by histone acetyltransferases in cardiomyocytes (Zhang *et al.* 2002). Moreover, dynamic regulation of other histone modifications has been demonstrated in cardiac myocytes (Illi *et al.* 2005; Bingham *et al.* 2007).

It remains to be established, however, (i) which epigenetic marks are dysregulated in association with heart failure *in vivo*, (ii) which regions of the human genome are susceptible to such epigenetic changes, and (iii) how epigenetic dysregulation affects the expression of protein-coding or other genes. To address these issues, we have now studied an animal model of congestive heart failure (CHF), the Dahl salt-sensitive rat (Rapp *et al.* 1989), and found that two histone modifications are markedly affected in cardiac myocytes during the development of CHF. We further confirmed our findings in human left ventricular (LV) myocytes with the use of chromatin immunoprecipitation

Communicated by: Kohei Miyazono
**Correspondence*: hmano@jichi.ac.jp

DOI: 10.1111/j.1365-2443.2008.01252.x

(ChIP) coupled to pyrosequencing. Our results have revealed dynamic histone modifications in the vicinity of a subset of protein-coding genes in the human genome, which directly participate in regulation of the contraction of cardiac myocytes.

Results

Histone modifications in the heart of Dahl rats

We prepared LV myocytes from Dahl salt-sensitive rats, which are genetically intolerant to excessive salt intake (Rapp *et al.* 1989). A high-sodium diet thus induces systemic hypertension and cardiac hypertrophy in Dahl rats within a few weeks. These changes are followed within a few months by the development of CHF and death. We isolated cardiac myocytes from rats with CHF (fed a high-sodium diet) as well as from age-matched animals with a normal heart (fed a low-sodium diet), and we subjected these cells to ChIP with antibodies to acetylated histone H3 (H3Ac), acetylated histone H4 (H4Ac), histone H3 dimethylated on lysine-4 (K4DM), histone H3 trimethylated on lysine-4 (K4TM), histone H3 dimethylated on lysine-9 (K9DM), histone H3 trimethylated on lysine-9 (K9TM), histone H4 trimethylated on lysine-20 (K20TM), or histone H3 dimethylated on lysine-27 (K27DM). The ChIP products as well as cRNA prepared from the normal or failed hearts were then individually subjected to hybridization with high-density oligonucleotide microarrays (Affymetrix Rat Genome 230 2.0 GeneChip) originally developed for expression profiling of rat genes.

Pearson's correlation coefficient for the signal intensity of all probe sets with a "Present" call (by Affymetrix GCOS software) in the normal heart ($n = 13\ 914$) was 0.873 in the cRNA hybridizations for normal and failed hearts (Fig. 1), indicative of a strong correlation in the expression level of most genes between the two samples. Consistent with this observation, the signal intensity for all probe sets with a positive value in the H3Ac ChIP products from the normal heart ($n = 12\ 027$) was highly correlated between these products from normal and failed hearts ($r = 0.724$). A similar strong correlation between the two groups was observed for H4Ac.

Unexpectedly, however, despite the strong correlation ($r = 0.856$) apparent for K4DM, only a weak negative correlation ($r = -0.097$) was detected for the K4TM mark between normal and failed hearts, indicative of marked differences in the associated gene sets. Similarly, although a strong correlation was observed for K9DM ($r = 0.558$), a weak negative correlation ($r = -0.251$) was apparent for K9TM. Hybridization levels were positively correlated between normal and failed hearts for K20TM and K27DM.

Thus, among the epigenetic marks examined, K4TM and K9TM were the histone modifications most affected in heart failure. Although differences in functional roles and genomic distributions between K4DM and K4TM have been described (Santos-Rosa *et al.* 2002; Bernstein *et al.* 2005), little has been known of such differential roles for the methylation level of lysine-9 of histone H3.

K4TM and K9TM profiles in the human heart

We next attempted to identify the genomic regions associated with the K4TM and K9TM marks in human cardiac myocytes. ChIP products for K4TM or K9TM were prepared from a mixture of LV tissue specimens from four individuals with retained pumping function [LV ejection fraction (EF) of 65.5 ± 7.6%, mean ± SD] or from four individuals with CHF (LVEF of 19.8 ± 5.7%) caused by dilated cardiomyopathy (Table 1). The ChIP

Table 1 Clinical characteristics of the subjects who provided specimens for the study

	Sample ID	Disease	Age (years)	Sex	LVEF (%)
HighEF	PM 8	HVD (MSR, ASR)	59	F	65
	PM12	HVD (MSR)	73	F	58
	PM13	HVD (MS)	55	F	76
	PM14	HVD (MS)	62	F	63
CHF	LV13	DCM	52	M	17
	LV14	DCM	55	M	25
	LV18	DCM	57	M	13
	LV20	DCM	64	F	24

HVD, heart valvular disease; MS(R), mitral stenosis (and regurgitation); ASR, aortic stenosis and regurgitation; DCM, dilated cardiomyopathy; F, female; M, male.

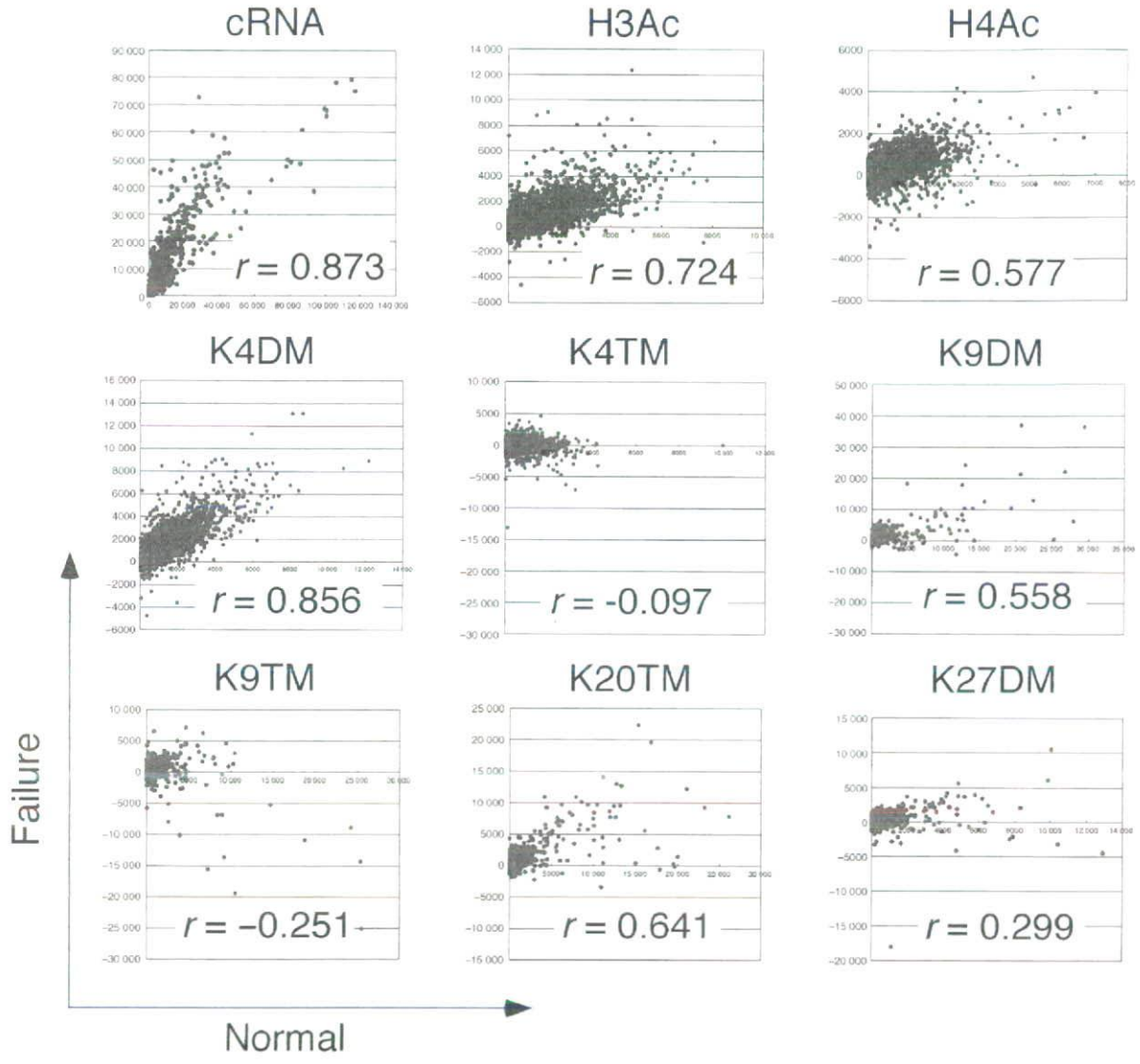

Figure 1 Comparison of epigenetic profiles between normal and failed rat hearts. The expression level of each probe set on oligonucleotide microarrays was compared between total cRNA from normal (*x* axis) or failed (*y* axis) hearts by calculation of Pearson's correlation coefficient (*r*). ChIP-on-chip data for H3Ac, H4Ac, K4DM, K4TM, K9DM, K9TM, K20TM, and K27DM are similarly compared.

products were subjected to pyrosequencing with the Genome Sequencer 20 system (Roche). In this "ChIP-to-seq" experiment, 96 069, 95 596, 116 267, and 96 734 reads were obtained for the K4TM products for specimens with retained LV ejection fraction (HighEF), the K4TM products for CHF, the K9TM products for HighEF, and the K9TM products for CHF, respectively. After quality-filtering, we isolated an average of 36 279 reads per sample, for each of which a single hit with a highest matching score was identified in the human genome sequence (the hg18 assembly of the Genome Bioinformatics Group, University of California at Santa Cruz) (Table S1 in Supporting Information). We thus focused on these reads for further analysis.

Many regions of the genome were identified in which multiple sequence reads mapped closely to each other. We therefore defined a "cluster" as a group of sequence reads localized within a distance of 1 kbp in the human genome (Fig. 2A). A total of 94 202 clusters was identified for all four samples, and 18 725 of these clusters, referred to as "high clusters," contained ≥ 2 sequence reads in ≥ 1 sample (see Table S2 in Supporting Information).

We then examined histone modification at the high clusters for specificity of the epigenetic mark (K4TM or

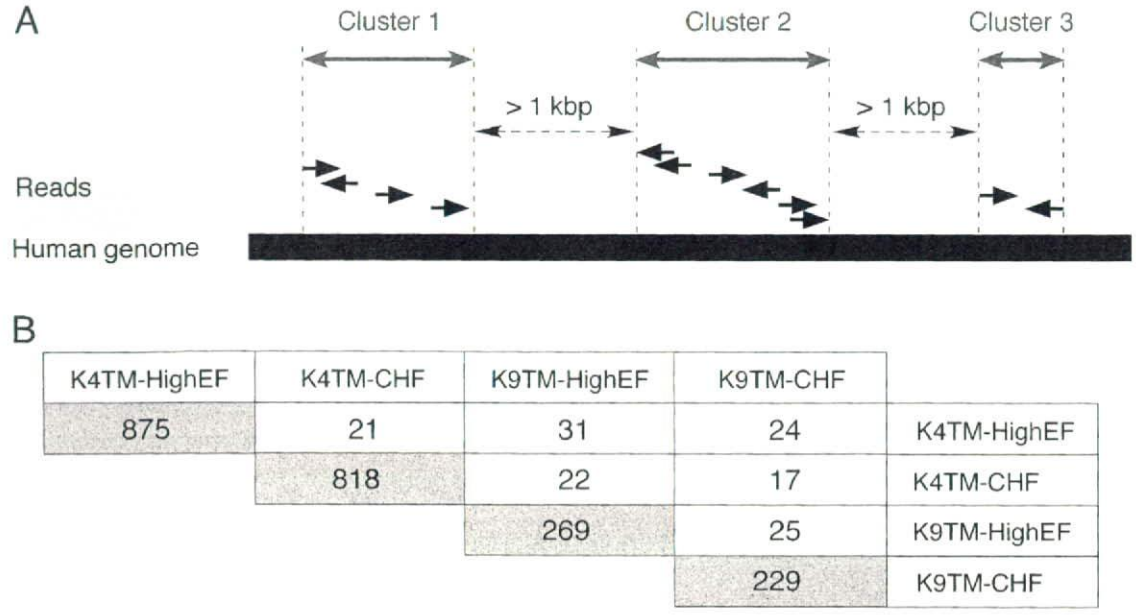

Figure 2 High clusters in K4TM and K9TM ChIP-to-seq data. (A) Groups of sequence reads that map to the human genome within a distance of 1 kbp are defined as "clusters," which are further denoted as "high clusters" when the read number in the cluster is ≥ 2 in ≥ 1 sample. (B) Numbers of high clusters with a read number of ≥ 5 for K4TM or K9TM in HighEF or CHF samples (shaded boxes). The numbers of such clusters shared between any pair of samples is also indicated (open boxes).

Table 2 Disease-specific high clusters

Mark	Characteristics of high clusters	Total number of high clusters	Number of high clusters close to RefSeq genes	Number of high clusters close to CpG islands
K4TM	HighEF ≥ 5, CHF ≤ 1	836	407	129
	HighEF ≤ 1, CHF ≥ 5	786	432	163
K9TM	HighEF ≥ 5, CHF ≤ 1	220	75	18
	HighEF ≤ 1, CHF ≥ 5	196	69	10

K9TM) and disease status (HighEF or CHF). Among the high clusters, 875 had ≥ 5 reads in the K4TM product for HighEF, 818 had ≥ 5 reads in the K4TM product for CHF, 269 had ≥ 5 reads in the K9TM product for HighEF, and 229 had ≥ 5 reads in the K9TM product for CHF (Fig. 2B). Only a few dozen of such high clusters were shared between any pair of samples, indicating the existence of disease-specific as well as methylation site-specific epigenetic profiles. Therefore, despite the heterogeneity in the cause of CHF (sustained systemic hypertension or dilated cardiomyopathy), both the Dahl rat and human data sets revealed a marked difference in the K4TM and K9TM epigenetic profiles between normal and failed hearts. Such specificity is further visualized for human chromosome 1 in Fig. S1 in Supporting Information. In contrast, the profile of read number per cluster was similar among the four groups of human ChIP products (see Fig. S2 in Supporting Information).

Genes mapped closely to disease-dependent clusters

We then isolated disease status-specific high clusters from the data set. A total of 836 high clusters was found to contain ≥ 5 reads in the K4TM products for HighEF but ≤ 1 read in those for CHF (HighEF-specific K4TM clusters); 407 RefSeq genes mapped to within ≤ 5 kbp of these clusters (Table 2). Similarly, 786 high clusters were found to be specific for K4TM and CHF (≤ 1 read in the K4TM products for HighEF but ≥ 5 reads in those for CHF). Smaller numbers of disease-dependent clusters were identified for the K9TM mark (220 HighEF-specific and 196 CHF-specific). These disease-dependent clusters

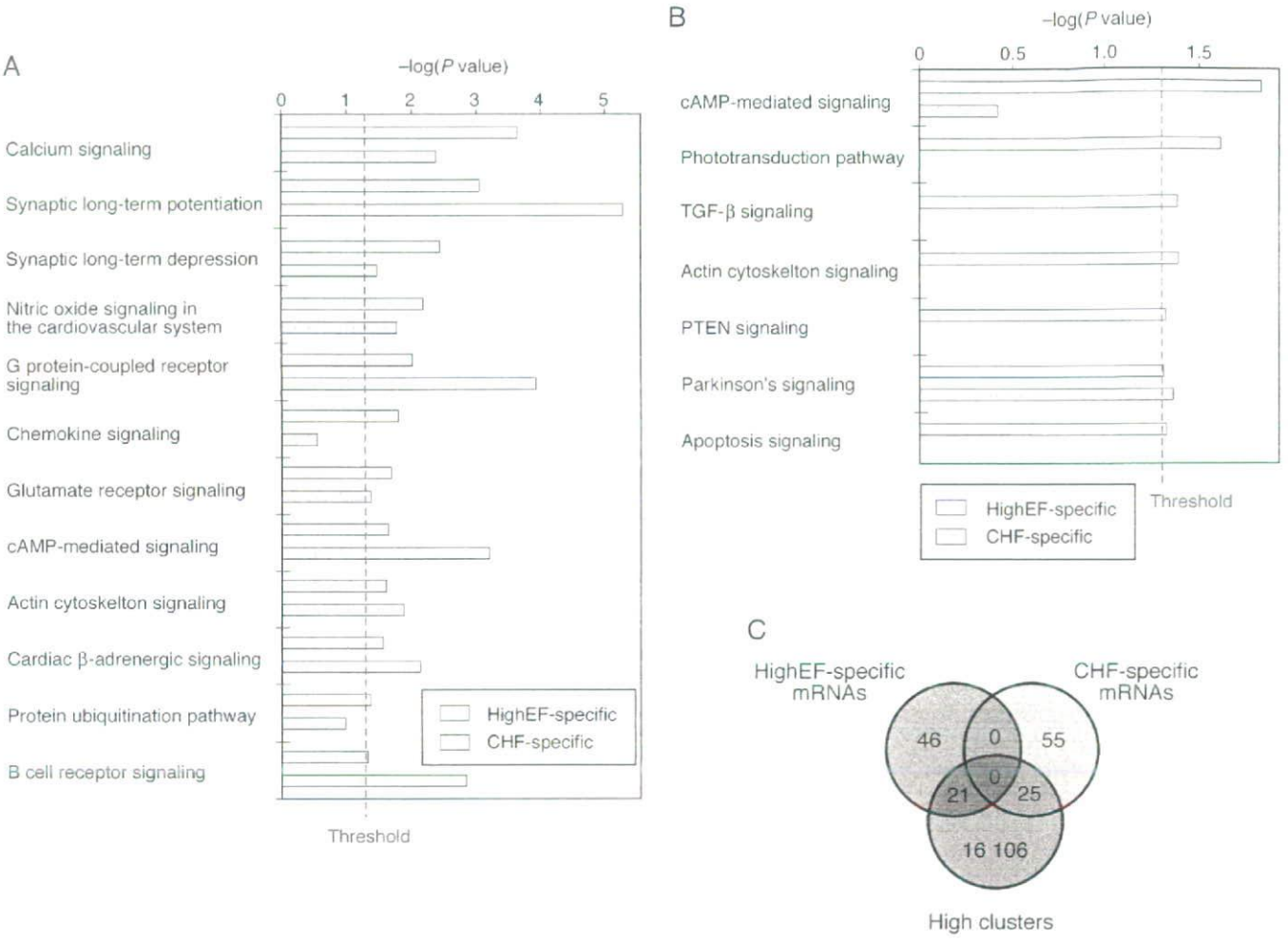

Figure 3 Analysis of genes that map in the vicinity of disease-dependent high clusters. (A) Canonical signaling pathways overrepresented in the HighEF-specific or CHF-specific high clusters for the K4TM ChIP products are listed with the corresponding −log(*P* value) score. (B) Canonical signaling pathways overrepresented in the HighEF-specific or CHF-specific high clusters for the K9TM ChIP products are listed with the corresponding −log(*P* value) score. (C) Venn diagram for comparison of transcripts associated specifically with HighEF or CHF status and those encoded by genes that map within a distance of < 5 kbp relative to a high cluster.

were widely distributed throughout human chromosomes and showed little overlap (see Fig. S3 in Supporting Information).

We examined whether the protein products of RefSeq genes that mapped in the vicinity (a distance of ≤ 5 kbp) of disease-dependent clusters function in canonical intracellular signaling pathways with the use of Ingenuity Pathway Analysis software (Ingenuity Systems; http://www.ingenuity.com). Analysis of the RefSeq genes associated with the disease-dependent K4TM clusters identified 12 canonical pathways that were significantly overrepresented ($P < 0.05$, Fisher's exact test) in HighEF-specific clusters and 20 pathways overrepresented in CHF-specific clusters. Many of the pathways ($n = 10$) were overrepresented in both HighEF-K4TM and CHF-K4TM clusters, almost all of which (including those for calcium signaling, synaptic long-term regulation, and nitric oxide signaling) are related to cardiac function (Fig. 3A).

Consistent with the disease-dependent selection of the clusters, the HighEF-associated and CHF-associated genes were distinct even within the same pathways. The canonical pathway for synaptic long-term potentiation, for example, contains the products of eight HighEF-associated and 12 CHF-associated genes, the interactions among which are shown in Fig. S4 in Supporting Information. Although genes corresponding to the calmodulin complex are present in both gene sets, these genes differ between the HighEF set (*CALM1*) and the CHF set (*CALM3*).

In addition to the proteins of the canonical signaling pathways, many products of the genes in the vicinity of disease-dependent high clusters for K4TM are functionally or physically networked. One such network comprises 34 proteins, 18 of which are encoded by HighEF-associated genes and 16 by CHF-associated genes (Fig. S5 in Supporting Information). Again, the genes for some complexes associated with both gene sets are distinct; those for the ATPase complex, for instance, include that for ATP1B1 in the HighEF-associated set and that for ATP5C1 in the CHF-associated set. Gene products in this network are substantially enriched in those implicated in cardiovascular disease.

In contrast to the K4TM-specific clusters, only a few canonical signaling pathways are linked to the RefSeq genes localized in the vicinity of K9TM-specific clusters. This difference is due in part to the small number of high clusters that contain disease-dependent reads for K9TM. Whereas the numbers of high clusters for HighEF specimens were similar between K4TM and K9TM products ($n = 6547$ and 5594, respectively), the numbers of disease-dependent clusters for the K9TM mark were only approximately 25% of those for the K4TM mark (Table 2). Seven canonical signaling pathways were over-represented ($P < 0.05$, Fisher's exact test) in the genes associated with the HighEF-K9TM clusters, whereas only one such pathway was overrepresented in those associated with the CHF-K9TM clusters (Fig. 3B). The network containing the most disease-dependent K9TM-associated gene products is centered on transforming growth factor β1 (TGFB1) and the tumor suppressor p53 (TP53), implicating K9TM-related regulation in cell death in the heart (see Fig. S6 in Supporting Information).

Our analysis thus revealed differential regulation of K4TM modification for genes related to cardiac function. To examine whether such epigenetic regulation plays a direct role in gene transcription, we performed gene expression profiling with Human Genome U133 Plus 2.0 arrays (Affymetrix) for the individual specimens (four for HighEF and four for CHF) used in the ChIP experiments. From the data obtained for 54 675 probe sets and the eight specimens, we selected HighEF-specific probe sets according to the following criteria: (i) the ratio of the mean expression level between HighEF and CHF was ≥ 3, and (ii) the mean expression level in HighEF was ≥ 10 arbitrary units (U). These criteria resulted in the isolation of 67 probe sets (see Table S3 in Supporting Information). CHF-specific probe sets were also selected on the basis of a CHF/HighEF ratio for mean expression level of ≥ 3 and a mean expression level in CHF of ≥ 10 U, resulting in the identification of 80 probe sets (see Table S4 in Supporting Information). A total of

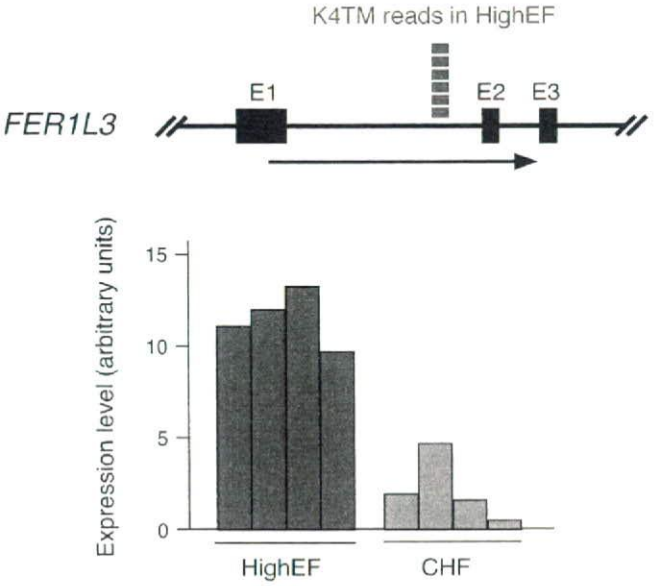

Figure 4 Epigenetic profile and mRNA abundance for *FER1L3*. Six sequence reads were selectively identified in the first intron of the *FER1L3* gene for the K4TM ChIP products of the HighEF sample (upper panel). E, exon. Consistent with this epigenetic profile, the amount of *FER1L3* mRNA was higher in the HighEF specimens than in the CHF specimens, as judged from the microarray data (lower panel).

16 152 of the transcripts measured with the U133 Plus 2.0 arrays mapped within a distance of ≤ 5 kbp relative to the high clusters. A Venn diagram revealed that only 21 probe sets were shared between the HighEF-specific and high cluster–associated transcripts, whereas 25 probe sets were shared between the CHF-specific and high cluster–associated transcripts (Fig. 3C). The K4TM mark has been found to map preferentially to the transcription start sites of active genes (Bernstein *et al.* 2005). Although a typical correlation between the K4TM modification and selective gene expression was apparent for a subset of genes (Fig. 4), our results suggest that this dynamic epigenetic regulation in the heart may not always directly participate in transcriptional regulation of neighboring genes.

Discussion

In the present study, we have revealed heart failure–dependent changes in the epigenetic profiles for K4TM and K9TM marks. The antibodies used in this study have been utilized in other reports for ChIP experiments, with those for K4TM and K9TM being especially employed in a genome-wide epigenetic profiling (Pokholok *et al.* 2005; Vakoc *et al.* 2006). Although it is difficult to

extensively verify our data in this study (because of the lack of knowledge in epigenetic profiles in heart), our ChIP procedure could faithfully confirm the epigenetic data demonstrated in previous studies [You *et al.* have, for instance, revealed that an apicidin treatment decreases the K4TM level while increases the K9TM level in the exon 1 of *DNMT1* in HeLa cells (You *et al.* 2008), and we could observe similar changes in the same experiment (data not shown)], supporting the reliability of our ChIP procedures.

Despite increasing evidence for a role of histone acetylation-deacetylation in the development of cardiac hypertrophy and heart failure, little information has been available for other histone modifications in these conditions (Illi *et al.* 2005; Phan *et al.* 2005; Bingham *et al.* 2007). Given the marked differences between the profiles of dimethylation and trimethylation for both K4 and K9 sites of histone H3, such trimethylation is likely under strict regulation in failed hearts.

The genes positioned close to the K4TM or K9TM marks were highly enriched in those that encode components of signaling pathways related to cardiac function. The HighEF-specific K4TM modification was, for instance, associated with *RYR2*, *CACNA2D1*, and *CACNB2* genes, the products of which directly participate in the regulation of intracellular calcium concentration and in muscle contraction (Cataldi *et al.* 1999; Marx *et al.* 2000). However, such disease-dependent histone methylation was not always linked to the induction or repression of neighboring genes. The expression level of the above three genes thus did not differ significantly between HighEF and CHF specimens (data not shown). Furthermore, only ~30% of HighEF- or CHF-specific transcripts were derived from genes associated with disease-dependent K4TM or K9TM modification (Fig. 3C). Consistent with such observations, the expression ratio for probe sets between normal and failed hearts of Dahl rats was not significantly correlated with the intensity ratio for any of the examined histone modifications, including H3Ac and H4Ac (data not shown). Therefore, despite the marked association between disease status and both transcript abundance and a subset of histone modifications, none of the latter can directly account for the former.

The epigenetic changes associated with heart failure may regulate gene transcription not through a single modification but through a combination of various marks (the "histone code" hypothesis) (Strahl & Allis 2000). The disease-dependent epigenetic changes also may alter the conformation of chromosomes, inducing an open or closed chromatin structure that indirectly affects the targets of subsequent regulation, such as the binding of transcription factors or additional chromatin remodeling. The subsequent regulation step would then play an important role in transcription of neighboring genes. In either case, our epigenetic profiles should facilitate further investigations into the roles of epigenetic changes in the development of heart failure.

Experimental procedures

ChIP-on-chip experiments

Dahl salt-sensitive rats (Japan SLC) at 6 weeks of age were maintained on a low-sodium diet (0.3% NaCl) or switched to a high-sodium diet (8% NaCl); the latter animals developed heart failure, as detected by echocardiography, after 13 weeks, as described previously (Ueno *et al.* 2003). ChIP products were prepared from the LV myocytes of 19-week-old Dahl rats with antibodies specific to H3Ac (Upstate, #17-245), H4Ac (Upstate, #17-229), K4DM (Abcam, #ab7766), K4TM (Abcam, #ab8580), K9DM (Upstate, #07-441), K9TM (Upstate, #07-442), K20TM (Abcam, #ab9053) or K27DM (Upstate, #07-452). The products were amplified by T7 RNA polymerase and subjected to hybridization with Affymetrix Rat Genome 230 2.0 microarrays as described previously (Takayama *et al.* 2007). Total genomic DNA (Pre-ChIP) and cRNA prepared from the LV tissue were also hybridized to the same arrays. The mean expression intensity of all probe sets was set to 500 U in each hybridization, and the fluorescence intensity of each test gene was normalized accordingly. Microarray data for rat and human hearts are available at the Gene Expression Omnibus web site (http://www.ncbi.nlm.nih.gov/geo) under the accession numbers GSE8341 and GSE8331, respectively. For the ChIP data, the signal intensity of each probe set in the Pre-ChIP analysis was then subtracted from that of the corresponding probe set in each ChIP experiment.

ChIP-to-seq experiments

All clinical specimens were obtained with written informed consent, and the study was approved by the ethics committees of Jichi Medical University and Hayama Heart Center. ChIP products were prepared from pooled samples for HighEF or CHF (each derived from four specimens) with antibodies to K4TM or K9TM. The products were converted to cRNA and amplified as described above for ChIP-on-chip experiments. The cRNA was then used to generate double-stranded DNA, which was subjected to pyrosequencing with a Genome Sequencer 20 system (Roche Diagnostics). Keypass wells occupied 82.7% to 87.0% of original Raw wells. Homology searches with the BLAST program were performed against the human genome sequence (the hg18 assembly) for each readout with the following parameter set: –e 2e-19 –v 50 –b 500 –T F –F F –m 8.

Acknowledgements

This work was supported in part by a Grant-in-Aid for Scientific Research on Priority Areas (C) "Medical Genome Science" from the

Ministry of Education, Culture, Sports, Science and Technology of Japan and by a grant (#04C7) from Salt Science Research Foundation (Tokyo, Japan).

References

Bernstein, B.E., Kamal, M., Lindblad-Toh, K., Bekiranov, S., Bailey, D.K., Huebert, D.J., McMahon, S., Karlsson, E.K., Kulbokas, E.J. 3rd, Gingeras, T.R., Schreiber, S.L. & Lander, E.S. (2005) Genomic maps and comparative analysis of histone modifications in human and mouse. *Cell* **120**, 169–181.

Bingham, A.J., Ooi, L., Kozera, L., White, E. & Wood, I.C. (2007) The repressor element 1-silencing transcription factor regulates heart-specific gene expression using multiple chromatin-modifying complexes. *Mol. Cell. Biol.* **27**, 4082–4092.

Braunwald, E. (1997) Shattuck lecture—cardiovascular medicine at the turn of the millennium: triumphs, concerns, and opportunities. *N. Engl. J. Med.* **337**, 1360–1369.

Cataldi, M., Secondo, A., D'Alessio, A., Taglialatela, M., Hofmann, F., Klugbauer, N., Di Renzo, G. & Annunziato, L. (1999) Studies on maitotoxin-induced intracellular $Ca^{(2+)}$ elevation in Chinese hamster ovary cells stably transfected with cDNAs encoding for L-type $Ca^{(2+)}$ channel subunits. *J. Pharmacol. Exp. Ther.* **290**, 725–730.

Gusterson, R.J., Jazrawi, E., Adcock, I.M. & Latchman, D.S. (2003) The transcriptional co-activators CREB-binding protein (CBP) and p300 play a critical role in cardiac hypertrophy that is dependent on their histone acetyltransferase activity. *J. Biol. Chem.* **278**, 6838–6847.

Iezzi, S., Di Padova, M., Serra, C., Caretti, G., Simone, C., Maklan, E., Minetti, G., Zhao, P., Hoffman, E.P., Puri, P.L. & Sartorelli, V. (2004) Deacetylase inhibitors increase muscle cell size by promoting myoblast recruitment and fusion through induction of follistatin. *Dev. Cell* **6**, 673–684.

Illi, B., Scopece, A., Nanni, S., Farsetti, A., Morgante, L., Biglioli, P., Capogrossi, M.C. & Gaetano, C. (2005) Epigenetic histone modification and cardiovascular lineage programming in mouse embryonic stem cells exposed to laminar shear stress. *Circ. Res.* **96**, 501–508.

James, M.A., Saadeh, A.M. & Jones, J.V. (2000) Wall stress and hypertension. *J. Cardiovasc. Risk* **7**, 187–190.

Kuwahara, K., Saito, Y., Ogawa, E., Takahashi, N., Nakagawa, Y., Naruse, Y., Harada, M., Hamanaka, I., Izumi, T., Miyamoto, Y., Kishimoto, I., Kawakami, R., Nakanishi, M., Mori, N. & Nakao, K. (2001) The neuron-restrictive silencer element-neuron-restrictive silencer factor system regulates basal and endothelin 1-inducible atrial natriuretic peptide gene expression in ventricular myocytes. *Mol. Cell. Biol.* **21**, 2085–2097.

Marx, S.O., Reiken, S., Hisamatsu, Y., Jayaraman, T., Burkhoff, D., Rosemblit, N. & Marks, A.R. (2000) PKA phosphorylation dissociates FKBP12.6 from the calcium release channel (ryanodine receptor): defective regulation in failing hearts. *Cell* **101**, 365–376.

Phan, D., Rasmussen, T.L., Nakagawa, O., McAnally, J., Gottlieb, P.D., Tucker, P.W., Richardson, J.A., Bassel-Duby, R. & Olson, E.N. (2005) BOP, a regulator of right ventricular heart development, is a direct transcriptional target of MEF2C in the developing heart. *Development* **132**, 2669–2678.

Pokholok, D.K., Harbison, C.T., Levine, S., Cole, M., Hannett, N.M., Lee, T.I., Bell, G.W., Walker, K., Rolfe, P.A., Herbolsheimer, E., Zeitlinger, J., Lewitter, F., Gifford, D.K. & Young, R.A. (2005) Genome-wide map of nucleosome acetylation and methylation in yeast. *Cell* **122**, 517–527.

Rapp, J.P., Wang, S.M. & Dene, H. (1989) A genetic polymorphism in the renin gene of Dahl rats cosegregates with blood pressure. *Science* **243**, 542–544.

Santos-Rosa, H., Schneider, R., Bannister, A.J., Sherriff, J., Bernstein, B.E., Emre, N.C., Schreiber, S.L., Mellor, J. & Kouzarides, T. (2002) Active genes are tri-methylated at K4 of histone H3. *Nature* **419**, 407–411.

Strahl, B.D. & Allis, C.D. (2000) The language of covalent histone modifications. *Nature* **403**, 41–45.

Takayama, K., Kaneshiro, K., Tsutsumi, S., Horie-Inoue, K., Ikeda, K., Urano, T., Ijichi, N., Ouchi, Y., Shirahige, K., Aburatani, H. & Inoue, S. (2007) Identification of novel androgen response genes in prostate cancer cells by coupling chromatin immunoprecipitation and genomic microarray analysis. *Oncogene* **26**, 4453–4463.

Ueno, S., Ohki, R., Hashimoto, T., Takizawa, T., Takeuchi, K., Yamashita, Y., Ota, J., Choi, Y.L., Wada, T., Koinuma, K., Yamamoto, K., Ikeda, U., Shimada, K. & Mano, H. (2003) DNA microarray analysis of *in vivo* progression mechanism of heart failure. *Biochem. Biophys. Res. Commun.* **307**, 771–777.

Vakoc, C.R., Sachdeva, M.M., Wang, H. & Blobel, G.A. (2006) Profile of histone lysine methylation across transcribed mammalian chromatin. *Mol. Cell. Biol.* **26**, 9185–9195.

You, J.S., Kang, J.K., Lee, E.K., Lee, J.C., Lee, S.H., Jeon, Y.J., Koh, D.H., Ahn, S.H., Seo, D.W., Lee, H.Y., Cho, E.J. & Han, J.W. (2008) Histone deacetylase inhibitor apicidin downregulates DNA methyltransferase 1 expression and induces repressive histone modifications via recruitment of corepressor complex to promoter region in human cervix cancer cells. *Oncogene* **27**, 1376–1386.

Zhang, C.L., McKinsey, T.A., Chang, S., Antos, C.L., Hill, J.A. & Olson, E.N. (2002) Class II histone deacetylases act as signal-responsive repressors of cardiac hypertrophy. *Cell* **110**, 479–488.

Received: 26 June 2008
Accepted: 10 October 2008

Supporting Information/Supplementary materials

The following Supporting Information can be found in the online version of the article:

Figure S1 Distribution of K4TM and K9TM marks on chromosome 1.

Figure S2 Distribution of read number per cluster in ChIP products.

Figure S3 Chromosome distribution of disease-specific high clusters.

Figure S4 Protein complexes in the synaptic long-term potentiation pathway in Fig. 3A are colored red or green on the basis of whether the corresponding genes are associated with HighEF-specific or CHF-specific high clusters for K4TM, respectively.

Figure S5 Interaction map for a protein network that contains the products of 18 and 16 genes associated with the HighEF-specific and CHF-specific high clusters for K4TM, respectively.

Figure S6 Network for the products of genes that mapped in the vicinity of K9TM high clusters.

Table S1 Output of pyrosequencing.

Table S2 High clusters identified in the heart specimens.

Table S3 Expression intensity of HighEF-specific probe sets.

Table S4 Expression intensity of CHF-specific probe sets.

Additional Supporting Information may be found in the online version of the article.

Please note: Wiley-Blackwell are not responsible for the content or functionality of any supporting information supplied by the authors. Any queries (other than missing material) should be directed to the corresponding author for the article.

Environ Health Prev Med (2008) 13:25–29
DOI 10.1007/s12199-007-0007-8

Epigenetic abnormalities in cardiac hypertrophy and heart failure

Hiroyuki Mano

Received: 23 June 2007 / Accepted: 4 August 2007 / Published online: 11 December 2007

Abstract Epigenetics refers to the heritable regulation of gene expression through modification of chromosomal components without an alteration in the nucleotide sequence of the genome. Such modifications include methylation of genomic DNA as well as acetylation, methylation, phosphorylation, ubiquitination, and SUMOylation of core histone proteins. Recent genetic and biochemical analyses indicate that epigenetic changes play an important role in the development of cardiac hypertrophy and heart failure, with dysregulation in histone acetylation status, in particular, shown to be directly linked to an impaired contraction ability of cardiac myocytes. Although such epigenetic changes should eventually lead to alterations in the expression of genes associated with the affected histones, little information is yet available on the genes responsible for the development of heart failure. Current efforts of our and other groups have focused on deciphering the network of genes which are under abnormal epigenetic regulation in failed hearts. To this end, coupling chromatin immunoprecipitation to high-throughput profiling systems is being applied to cardiac myocytes in normal as well as affected hearts. The results of these studies should not only improve our understanding of the molecular basis for cardiac hypertrophy/heart failure but also provide essential information that will facilitate the development of new epigenetics-based therapies.

H. Mano (✉)
Division of Functional Genomics, Jichi Medical University, 3311-1 Yakushiji, Shimotsuke, Tochigi 329-0498, Japan
e-mail: hmano@jichi.ac.jp

Keywords Cardiac hypertrophy · Chromatin immunoprecipitation · Heart failure · Histone acetylation · Subtraction

What is "epigenetics"?

The eukaryotic genome is tightly compacted as a result of its association with highly conserved histone proteins. The interaction of stretches of genomic DNA with core histone proteins (two molecules each of H2A, H2B, H3, and H4) thus results in the formation of nucleosomes, which are the basic structural units of chromatin. The further association of histone H1 and other proteins with nucleosomes strengthens the compaction and gives rise to the highly ordered, condensed structure of the chromosome (Fig. 1). The interaction of genomic DNA with these chromosomal proteins greatly influences the access of transcriptional factors to their target DNA sequences and thereby regulates transcriptional activity.

"Epigenetics" refers to the heritable regulation of gene expression through the modification of chromosomal components without an alteration in the nucleotide sequence of the genome [1]. Several such modifications have been linked to the regulation of gene expression, including methylation of genomic DNA as well as acetylation, methylation, phosphorylation, ubiquitination, and sumoylation of histone proteins (Fig. 1).

Core histones have an amino-terminal tail that protrudes from the chromatin fiber and which is believed to interact with DNA or other histone or modulatory proteins. Lysine and arginine residues within this tail are the main targets for histone modification. Lysine-9 in histone H3 (H3-K9), for example, becomes methylated or acetylated in response to a variety of signals. In general, the acetylation of

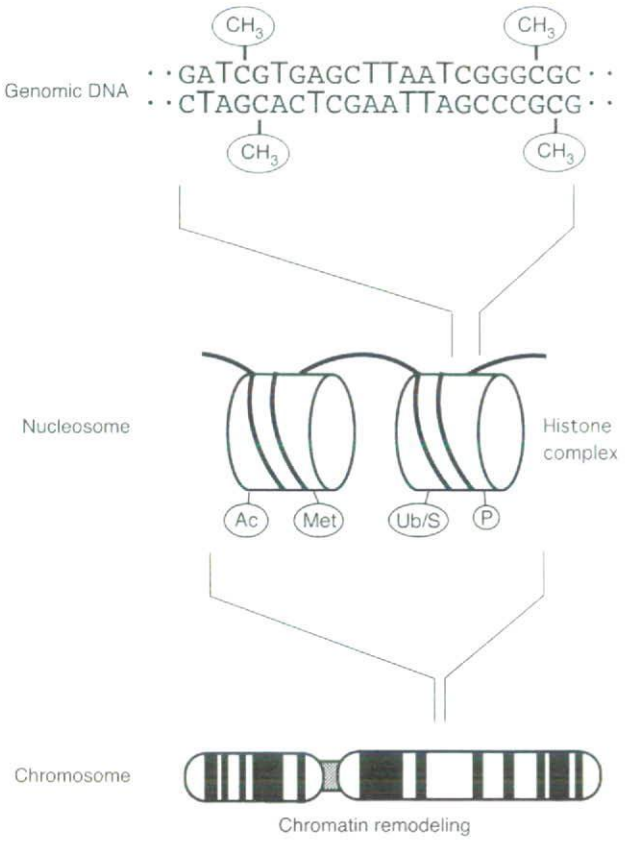

Fig. 1 Epigenetic changes at different levels of chromatin structure. CpG sites within genomic DNA undergo methylation, and core histones in nucleosomes undergo acetylation (*Ac*), methylation (*Met*), ubiquitination (*Ub*), sumoylation (*S*), or phosphorylation (*P*). Higher order chromatin structure is also dynamically modified by chromatin-remodeling complexes

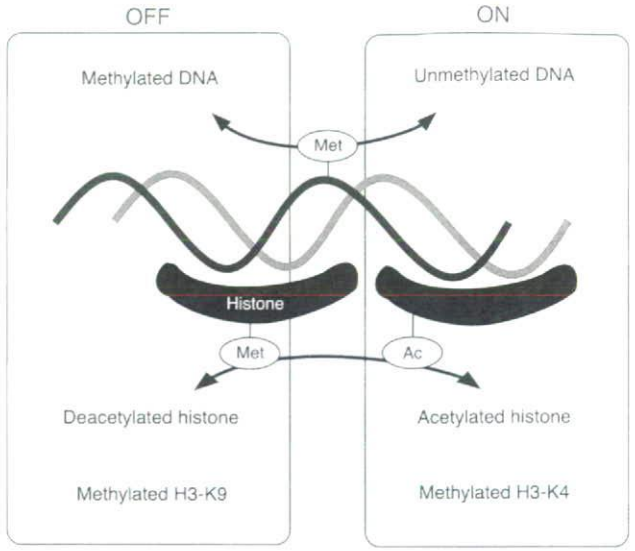

Fig. 2 Epigenetic changes and transcriptional activity. Suppression of gene expression (*OFF*) is correlated with the methylation (*Met*) of genomic DNA, deacetylation of histones, and methylation of H3-K9. In contrast, activation of gene expression (*ON*) is associated with unmethylated genomic DNA, acetylated (*Ac*) histones, and methylated H3-K4

histones is associated with the induction of gene expression (Fig. 2). The acetylation of histone tails is thought to neutralize the positive charge of lysine residues and thereby to induce a decondensation of chromatin structure. The resulting open architecture of the chromosome allows transcriptional factors to access their binding sites in genomic DNA and to activate transcription. However, the same histone modification has been associated with seemingly diverse outputs in a context-dependent manner. The existence of a "histone code" has thus been proposed, with a combination of histone modifications – and not only one – supposedly specifying the outcome in terms of gene expression [2]. However, this hypothesis has been challenged by recent data [3].

The acetylation of histone tails is mediated by histone acetyltransferases (HATs), whose activity in cells is rapidly counteracted by that of histone deacetylases (HDACs) [4]. The turnover time of histone acetylation in cells is thus as short as a few minutes [5]. The importance of histone acetylation in the regulation of gene expression has been demonstrated for a variety of cellular processes, including cell differentiation, cell cycle progression, DNA repair, and carcinogenesis [6, 7].

Epigenetic status in cardiac myocytes

The regulation of histone acetylation has been shown to be linked to cardiac hypertrophy. The HAT activity of CREB-binding protein (CBP) and p300 is thus required for the induction of hypertrophic changes in cardiac muscle cells by phenylephrine [8]. Consistent with this observation, the inhibition of HDAC activity results in an increase in the size of muscle cells [9]. Furthermore, class II HDACs (HDAC4, -5, -7, and -9) suppress cardiac hypertrophy, in part by binding to and inhibiting the activity of myocyte enhancer factor 2 (MEF2) [10]. In contrast, however, HDAC2 together with Hop, a homeodomain protein, was found to promote cardiac hypertrophy in vivo in a manner sensitive to systemic administration of the HDAC inhibitor trichostatin A (TSA) [11]. Moreover, HDAC inhibitors prevent hypertrophy and sarcomere organization in cultured cardiac myocytes [12], which is suggestive of a positive role for HDACs in cardiac hypertrophy.

These seemingly discrepant findings may be attributable either to differential actions of different classes of HDACs (and, possibly, of HATs) with regard to myocyte hypertrophy or to a dissociation between the deacetylase activity of HDACs and a pro-hypertrophic function [10]. Clarification of the role of HATs and HDACs in hypertrophy

would be facilitated by the identification of the genes targeted by these enzymes during the induction of hypertrophic changes. Little is known, however, of the genes regulated by HATs or HDACs in myocytes. Induction of the atrial natriuretic peptide (ANP) gene is associated with the acetylation of histones (H3 and H4) located in the 3′ untranslated region of the gene [13]. Histones bound to the β-myosin heavy chain gene have also been shown to be targeted by HATs in myocytes [10].

Differential chromatin scanning (DCS) method

Given the essential role of histone acetylation in cardiac hypertrophy, it is important that the genes or genome regions bound to histones with such differential modifications be identified. Chromatin immunoprecipitation (ChIP) coupled with hybridization to genome tiling microarrays ("ChIP-on-chip" experiments) has been used to screen for those genes under epigenetic regulation [14–16]. However, an extensive mapping of ChIP products on the human genome has been hampered by insufficient information on human genome annotation. Furthermore, hybridization of genome-derived fragments to microarrays is prone to non-specific signals that partly represent the GC contents of the fragments.

To effectively isolate genome fragments with differential epigenetic regulation, we have developed a novel "DCS" method which basically couples ChIP to subtraction PCR [17, 18]. The DCS procedure is schematically shown in Fig. 3. Following the cross-linking of DNA to histones through the use of formaldehyde, both tester and driver cells are separately lysed and subjected to mild DNA shearing by sonication for a short period. Complexes of DNA and acetylated histones are then specifically immunoprecipitated with antibodies to acetylated histone H3, after which the DNA fragments are released from such complexes into solution.

The nonspecific binding of residual RNA is then minimized by treating the DNA solution with RNase A, and the DNA fragments are then blunt-ended. The DNA is digested maximally with *Rsa*I to obtain fragments with a relatively uniform size of several hundred base pairs. A TAG adaptor is ligated to both ends of the DNA fragments, and subsequent PCR amplification with a TAG primer yields amplicons with an *Xma*I/*Sma*I site at each end.

The tester DNA is then digested with *Xma*I (thereby generating cohesive ends), whereas the driver DNA is digested with *Sma*I (generating blunt ends). The tester DNA is ligated with the first subtraction adaptor [19] at its cohesive ends and is then annealed to an excess amount of the driver DNA. Under this condition, DNA fragments present only in the tester sample undergo self-annealing and thereby generate a binding site for the first subtraction

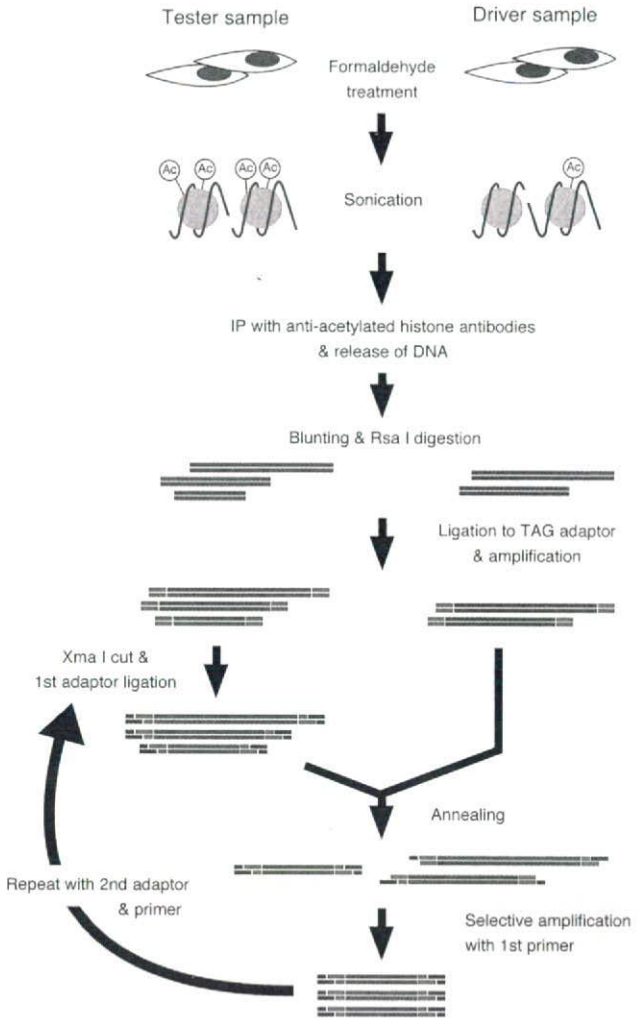

Fig. 3 The differential chromatin scanning (DCS) method. DNA fragments bound to acetylated (*Ac*) histones are purified by immunoprecipitation (*IP*) and subjected to TAG adaptor ligation (*green bars*) and PCR amplification. The tester DNA is then digested with *Xma*I, ligated to the first subtraction adaptor (*red bars*), and annealed with an excess amount of the driver DNA. Given that only the tester-specific fragments self-anneal, PCR with the first subtraction primer selectively amplifies these fragments. The products are subjected to a second round of subtraction PCR with the second subtraction adaptor and primer to ensure the fidelity of the subtraction. Reproduced from Kaneda et al. [17]

primer at both ends. Subsequent PCR amplification with this primer thus selectively amplify the tester-specific DNA fragments [17].

To exclude DNA fragments that possess endogenous (probably nonspecific) binding sites for the first subtraction primer, we then digest the first subtraction products with *Xma*I and ligate the resulting molecules with the second subtraction adaptor. A second round of subtraction amplification is then performed with the second subtraction primer, yielding DNA fragments that are associated with acetylated histones, specifically in the tester cells [17].

To verify the fidelity of DCS, we attempted to isolate genome fragments which are the targets of HDAC in cardiac myocytes. A rat cardiomyocyte cell line, H9C2, was treated with TSA and was used as the tester, while the cells without the TSA treatment was used as the driver. Differential chromatin scanning was applied to this pair of cells and subsequently identified hundreds of genome fragments that could be immunoprecipitated by antibodies to acetylated histones only in the tester cells.

Some of the clones thus identified correspond to loci within or close to rat genes whose products function in intracellular calcium mobilization or antioxidant processes. One such clone, H9C2T-2_D09, mapped to a region encompassing intron 21 and exon 22 of *Itpr3* (Fig. 4a), which encodes a receptor for inositol 1,4,5-trisphosphate that plays an important role in Ca^{2+}-mediated signal transduction [18]. The cytosolic concentration of Ca^{2+} directly regulates muscle contraction and cardiac rhythm and is a determinant of myocyte hypertrophy and heart failure [20]. The amount of the genomic fragment corresponding to the H9C2T-2_D09 clone was 6.6-fold greater in the ChIP product of TSA-treated cells than in that of untreated cells (Fig. 4b), indicating that the extent of histone acetylation in this region of the genome of the tester cells was 6.6-fold that in the driver cells. Furthermore, inhibition of HDAC activity was accompanied by an increase in the amount of *Itpr3* mRNA [18] (Fig. 4c). These data suggest that HDAC actively deacetylates a chromosomal region corresponding to *Itpr3* and thereby suppresses the transcriptional activity of the gene.

To visualize directly the genome-wide distribution of HDAC targets, we mapped the DCS genomic clones whose chromosomal positions were known to rat chromosome figures (Fig. 5). The HDAC targets were distributed widely throughout the rat genome, although some "hot spots" for deacetylation were apparent. For example, seven of the DCS clones mapped to chromosomal position 5q36, and detailed mapping revealed that all of these clones were located within a region spanning 27 Mbp. It is thus possible that regional alterations of chromatin structure result in coordinated transcriptional regulation of genes within the affected region.

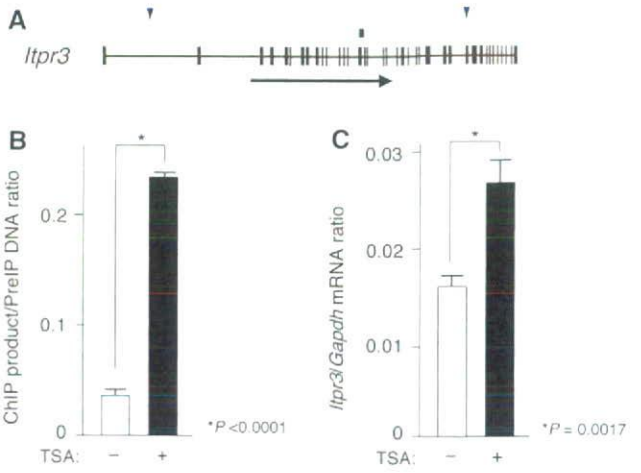

Fig. 4 Identification of *Itpr3* as a target of histone deacetylase (HDAC) in cardiomyocytes. **a** One of the DCS clones (H9C2T-2_D09; *red rectangle*) was mapped to chromosome 20p12, spanning intron 21 and exon 22 of *Itpr3*. Exons are denoted by *black boxes*, the *arrow* indicates the direction of transcription, and *blue triangles* depict distance markers separated by 50 kbp. **b** Chromatin immunoprecipitates were prepared from H9C2 cells treated (+) or not (−) with 300 n*M* inhibitor trichostatin A (TSA) for 24 h. The amount of DNA corresponding to the H9C2T-2_D09 sequence in each chromatin immunoprecipitation (*ChIP*) product relative to that in the corresponding original sample before immunoprecipitation (*PreIP*) was then determined by real-time PCR. **c** The amount of *Itpr3* mRNA relative to that of *Gapdh* mRNA in H9C2 cells treated or not with TSA was determined by quantitative reverse transcription (RT)-PCR. All data are means ± SD of triplicates from representative experiments that were performed at least twice. *P* values for the indicated comparisons were determined by Student's *t* test. Reproduced from Kaneda et al. [18]

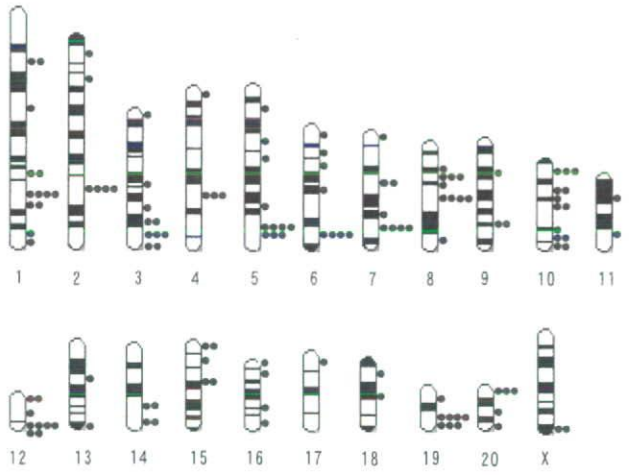

Fig. 5 Chromosomal distribution of HDAC targets. The genome fragments (*red dots*) isolated by the DCS method were mapped to rat chromosomes. Reproduced from Kaneda et al. [18]

Future directions

As described herein, cells manifest numerous types of epigenetic modifications, including acetylation and methylation, on core histone proteins. Although the results of biochemical and genetic studies suggest that histone acetylation plays an important role in the development of cardiac hypertrophy/heart failure (at least, in mouse), it is an open question whether changes in the other epigenetic marks are essential or, rather, causative of the heart disorders. An analysis of human heart specimens would be of particular great value.

In terms of technology development, DCS is not free from disadvantages. Although DCS can isolate genome fragments that are the recipients differential regulation of any epigenetic marks (provided specific antibodies are available), it does not measure the extent of "differential regulation". In other words, DCS is more a qualitative approach than a quantitative one. Several high-throughput sequencing technologies are currently emerging which simultaneously provide sequence information for millions of clones [21]. Coupling such sequencing system to ChIP would be one of the ideal ways to quantitatively measure epigenetic modifications: (1) frequency in the read data would be a surrogate marker for the intensity of epigenetic modifications; (2) sequence information of the reads would be useful to map such reads onto human genome.

It is apparent that epigenetic change is the key event in the development of cardiac hypertrophy/heart failure. Analysis of human specimens with emerging technologies would substantially facilitate researchers in their efforts to pinpoint the causative genes for these disorders.

References

1. Egger G, Liang G, Aparicio A, Jones PA. Epigenetics in human disease and prospects for epigenetic therapy. Nature. 2004;429:457–63.
2. Strahl BD, Allis CD. The language of covalent histone modifications. Nature. 2000;403:41–5.
3. Dion MF, Altschuler SJ, Wu LF, Rando OJ. Genomic characterization reveals a simple histone H4 acetylation code. Proc Natl Acad Sci USA. 2005;102:5501–6.
4. Verdin E, Dequiedt F, Kasler HG. Class II histone deacetylases: versatile regulators. Trends Genet. 2003;19:286–93.
5. Waterborg JH. Dynamics of histone acetylation in vivo. A function for acetylation turnover? Biochem Cell Biol. 2002;80:363–78.
6. Kouzarides T. Histone acetylases and deacetylases in cell proliferation. Curr Opin Genet Dev. 1999;9:40–8.
7. Yasui W, Oue N, Ono S, Mitani Y, Ito R, Nakayama H. Histone acetylation and gastrointestinal carcinogenesis. Ann NY Acad Sci. 2003;983:220–31.
8. Gusterson RJ, Jazrawi E, Adcock IM, Latchman DS. The transcriptional co-activators CREB-binding protein (CBP) and p300 play a critical role in cardiac hypertrophy that is dependent on their histone acetyltransferase activity. J Biol Chem. 2003;278:6838–47.
9. Iezzi S, Di Padova M, Serra C, Caretti G, Simone C, Maklan E, et al. Deacetylase inhibitors increase muscle cell size by promoting myoblast recruitment and fusion through induction of follistatin. Dev Cell. 2004;6:673–84.
10. Zhang CL, McKinsey TA, Chang S, Antos CL, Hill JA, Olson EN. Class II histone deacetylases act as signal-responsive repressors of cardiac hypertrophy. Cell. 2002;110:479–88.
11. Kook H, Lepore JJ, Gitler AD, Lu MM, Wing-Man Yung W, Mackay J, et al. Cardiac hypertrophy and histone deacetylase-dependent transcriptional repression mediated by the atypical homeodomain protein Hop. J Clin Invest. 2003;112:863–71.
12. Antos CL, McKinsey TA, Dreitz M, Hollingsworth LM, Zhang CL, Schreiber K, et al. Dose-dependent blockade to cardiomyocyte hypertrophy by histone deacetylase inhibitors. J Biol Chem. 2003;278:28930–7.
13. Kuwahara K, Saito Y, Ogawa E, Takahashi N, Nakagawa Y, Naruse Y, et al. The neuron-restrictive silencer element-neuron-restrictive silencer factor system regulates basal and endothelin 1-inducible atrial natriuretic peptide gene expression in ventricular myocytes. Mol Cell Biol. 2001;21:2085–97.
14. Weinmann AS, Yan PS, Oberley MJ, Huang TH, Farnham PJ. Isolating human transcription factor targets by coupling chromatin immunoprecipitation and CpG island microarray analysis. Genes Dev. 2002;16:235–44.
15. Ballestar E, Paz MF, Valle L, Wei S, Fraga MF, Espada J, et al. Methyl-CpG binding proteins identify novel sites of epigenetic inactivation in human cancer. EMBO J. 2003;22:6335–45.
16. Odom DT, Zizlsperger N, Gordon DB, Bell GW, Rinaldi NJ, Murray HL, et al. Control of pancreas and liver gene expression by HNF transcription factors. Science. 2004;303:1378–81.
17. Kaneda R, Toyota M, Yamashita Y, Koinuma K, Choi YL, Ota J, et al. High-throughput screening of genome fragments bound to differentially acetylated histones. Genes Cells. 2004;9:1167–74.
18. Kaneda R, Ueno S, Yamashita Y, Choi YL, Koinuma K, Takada S, et al. Genome-wide screening for target regions of histone deacetylases in cardiomyocytes. Circ Res. 2005;97:210–8.
19. Toyota M, Ho C, Ahuja N, Jair KW, Li Q, Ohe-Toyota M, et al. Identification of differentially methylated sequences in colorectal cancer by methylated CpG island amplification. Cancer Res. 1999;59:2307–12.
20. Marks AR. Cardiac intracellular calcium release channels: role in heart failure. Circ Res. 2000;87:8–11.
21. Service RF. Gene sequencing. The race for the $1000 genome. Science. 2006;311:1544–6.

Environ Health Prev Med (2008) 13:30–35
DOI 10.1007/s12199-007-0004-y

REVIEW

Epidemiological approach to nosocomial infection surveillance data: the Japanese Nosocomial Infection Surveillance System

Machi Suka · Katsumi Yoshida · Jun Takezawa

Received: 11 May 2007 / Accepted: 9 August 2007 / Published online: 11 December 2007

Abstract Surveillance of nosocomial infection is the foundation of infection control. Nosocomial infection surveillance data ought to be summarized, reported, and fed back to health care personnel for corrective action. Using the Japanese Nosocomial Infection Surveillance (JANIS) data, we determined the incidence of nosocomial infections in intensive care units (ICUs) of Japanese hospitals and assessed the impact of nosocomial infections on mortality and length of stay. We also elucidated individual and environmental factors associated with nosocomial infections, examined the benchmarking of infection rates and developed a practical tool for comparing infection rates with case-mix adjustment. The studies carried out to date using the JANIS data have provided valuable information on the epidemiology of nosocomial infections in Japanese ICUs, and this information will contribute to the development of evidence-based infection control programs for Japanese ICUs. We conclude that current surveillance systems provide an inadequate feedback of nosocomial infection surveillance data and, based on our results, suggest a methodology for assessing nosocomial infection surveillance data that will allow infection control professionals to maintain their surveillance systems in good working order.

Keywords Epidemiology · Intensive care units · Japan · Nosocomial infections · Surveillance

Introduction

Infection control in the hospital setting is performed with the aim of improving the effectiveness of patient care and promoting patient safety. Infection control professionals need to recognize and explain nosocomial infections and design and implement interventions to reduce their incidence. These infection control activities should have their bases in a well-designed surveillance system of nosocomial infections [1].

Compared with the USA and other developed countries, Japan traditionally had limited sources of information on the epidemiology of nosocomial infections and, until recently, little was known about the incidence and outcome of nosocomial infections in Japanese hospitals. The Japanese Ministry of Health, Labour, and Welfare established the Japanese Nosocomial Infection Surveillance (JANIS) system in July 2000, when participating hospitals routinely started to collect and subsequently make their nosocomial infection surveillance data available for entry into a national database. The JANIS database has now become the most important source of information on the epidemiology of nosocomial infections in Japanese hospitals.

In the study reported here, we used the JANIS data to determine the incidence of nosocomial infections in intensive care units (ICUs) of Japanese hospitals and assess the impact of nosocomial infections on mortality and length of stay. We elucidated individual and environmental

This article is based upon the research that was given encouragement award at the 77th annual meeting of the Japanese Society for Hygiene held in Osaka, Japan on 25–28 March 2007.

M. Suka (✉) · K. Yoshida
Department of Preventive Medicine, St Marianna University School of Medicine, 2-16-1 Sugao, Miyamae-ku Kawasaki, Kanagawa 216-8511, Japan
e-mail: suka@marianna-u.ac.jp

J. Takezawa
Department of Emergency and Intensive Care Medicine, Nagoya University Graduate School of Medicine, Nagoya, Japan

bjh research paper

Functional analysis of *JAK3* mutations in transient myeloproliferative disorder and acute megakaryoblastic leukaemia accompanying Down syndrome

Tomohiko Sato,[1] Tsutomu Toki,[1] Rika Kanezaki,[1] Gang Xu,[1] Kiminori Terui,[1] Hirokazu Kanegane,[2] Masayoshi Miura,[3] Souichi Adachi,[4] Masahiro Migita,[5] Shingo Morinaga,[6] Takahide Nakano,[7] Mikiya Endo,[8] Seiji Kojima,[9] Hitoshi Kiyoi,[10] Hiroyuki Mano[11] and Etsuro Ito[1]

[1]Department of Paediatrics, Hirosaki University Graduate School of Medicine, Hirosaki, [2]Department of Paediatrics, Graduate School of Medicine, University of Toyama, Toyama, [3]Department of Paediatrics, Toyama City Hospital, Toyama, [4]Department of Paediatrics, Graduate School of Medicine, Kyoto University, Kyoto, [5]Department of Paediatrics, Japan Red Cross Kumamoto Hospital, Kumamoto, [6]Department of Paediatrics, National Hospital Organization Kumamoto Medical Centre, Kumamoto, [7]Department of Paediatrics, Kansai Medical University, Osaka, [8]Department of Paediatrics, Iwate Medical University, Morioka, [9]Department of Paediatrics, Nagoya University Graduate School of Medicine, Nagoya, [10]Department of Infectious Diseases, Nagoya University Graduate School of Medicine, Nagoya, and [11]Division of Functional Genomics, Jichi Medical University, Shimotsuke, Japan

Summary

JAK3 mutations have been reported in transient myeloproliferative disorder (TMD) as well as in acute megakaryoblastic leukaemia of Down syndrome (DS-AMKL). However, functional consequences of the *JAK3* mutations in TMD patients remain undetermined. To further understand how *JAK3* mutations are involved in the development and/or progression of leukaemia in Down syndrome, additional TMD patients and the DS-AMKL cell line MGS were screened for *JAK3* mutations, and we examined whether each *JAK3* mutation is an activating mutation. *JAK3* mutations were not detected in 10 TMD samples that had not previously been studied. Together with our previous report we detected *JAK3* mutations in one in 11 TMD patients. Furthermore, this study showed for the first time that a TMD patient-derived *JAK3* mutation ($JAK3^{I87T}$), as well as two novel *JAK3* mutations ($JAK3^{Q501H}$ and $JAK3^{R657Q}$) identified in an MGS cell line, were activating mutations. Treatment of MGS cells and Ba/F3 cells expressing the JAK3 mutants with JAK3 inhibitors significantly decreased their growth and viability. These results suggest that the *JAK3* activating mutation is an early event during leukaemogenesis in Down syndrome, and they provide proof-of-principle evidence that JAK3 inhibitors would have therapeutic effects on TMD and DS-AMKL patients carrying activating *JAK3* mutations.

Keywords: Down syndrome, transient myeloproliferative disorder, acute megakaryoblastic leukaemia, JAK3, STAT5.

Received 14 November 2007; accepted for publication 2 January 2008

Correspondence: Etsuro Ito, Department of Paediatrics, Hirosaki University Graduate School of Medicine, Hirosaki, Aomori, 036-8563 Japan. E-mail: eturou@cc.hirosaki-u.ac.jp

Down syndrome (DS), which is caused by trisomy 21, is one of the most common human chromosomal abnormalities. Children with DS have an approximately 20-fold higher incidence of leukaemia than the general population (Hitzler & Zipursky, 2005). The majority of leukaemia cases associated with DS are acute megakaryoblastic leukaemia (AMKL). Approximately 10% of infants with DS develop a postnatal transient myeloproliferative disorder (TMD), which is characterized by rapid growth of abnormal blast cells with erythroid-megakaryocytic phenotype (Ito *et al*, 1995). Although the majority of TMD cases resolve spontaneously, AMKL develops in approximately 20% of TMD cases in the first four years of life. Recently, we and others demonstrated that acquired mutations of the *GATA1* gene were detected in almost all cases

 First published online 7 April 2008
British Journal of Haematology, **141**, 681–688 doi:10.1111/j.1365-2141.2008.07081.x